DEVELOPMENT OF AN IMPROVED SATELLITE IMAGERY METHOD FOR ESTIMATING THE CONSTRUCTION YEARS OF ROAD BRIDGES

道路橋の建設年を推定するための改良された衛星画像解析手法の開発

A dissertation submitted to the Division of Civil Engineering, Graduate School of Engineering, Hokkaido University in partial fulfillment of the requirements for the Degree of Doctor of Philosophy in Engineering

by
BENNIE HAMUNZALA

Examination Committee

Associate Professor Dr. Koji Matsumoto
Professor Dr. Kohei Nagai
Professor Dr. Takashi Matsumoto

Division of Civil Engineering
Faculty of Engineering
Hokkaido University
Sapporo, Japan

September 2024

Author's Address: Division of Civil Engineering, Faculty of Engineering,
Kita 8, Nishi 5, Kita-ku, Sapporo, Hokkaido, 060-0808
Hokkaido University
bennie.hamunzala.p8@elms.hokudai.ac.jp

Supervisor: Associate Professor Dr. Koji Matsumoto
Division of Civil Engineering, Faculty of Engineering,
Kita 8, Nishi 5, Kita-ku, Sapporo, Hokkaido, 060-0808
Hokkaido University
km312@eng.hokudai.ac.jp

Reviewers: Professor Dr. Kohei Nagai
Division of Civil Engineering, Faculty of Engineering,
Kita 8, Nishi 5, Kita-ku, Sapporo, Hokkaido, 060-0808
Hokkaido University
nagai325@eng.hokudai.ac.jp

Professor Dr. Takashi Matsumoto
Division of Civil Engineering, Faculty of Engineering,
Kita 8, Kita-ku Kita 13, Kita-ku, Sapporo, Hokkaido, 060-8628
Hokkaido University

ISBN xxx-xxx-xxxx-xx-x (printed)
ISSN xxxx-xxxx
Sapporo YYYY

ISBN xxx-xxx-xxxx-xx-x (pdf)
ISSN xxxx-xxxx
Sapporo YYYY

Acknowledgements

I am deeply grateful to God Almighty for granting me the opportunity to complete this study within the given timeframe.

I would like to express my heartfelt gratitude to my supervisor, Associate Professor Dr. Koji Matsumoto from the Laboratory of Engineering for Maintenance Systems at Hokkaido University, Japan. His guidance, support, constructive criticisms, and encouragement were invaluable throughout my tenure at the university. His expertise, wisdom, and patience helped me overcome various challenges and stay focused on my research. Dr. Matsumoto's commitment to excellence and his ability to provide insightful feedback were instrumental in shaping the direction and quality of my work. He consistently provided a supportive environment that allowed me to thrive academically and personally. I am forever grateful for his unwavering support, which extended beyond academic concerns, and his genuine interest in my overall well-being. His mentorship has had a profound impact on my professional development and will continue to influence my career for years to come.

I would also like to extend my sincere thanks to Professor Dr. Kohei Nagai from the Laboratory of Engineering for Maintenance Systems at Hokkaido University, Japan. His support, guidance, and constructive criticisms during the research presentations and journal preparation were extremely helpful. His insights and feedback significantly contributed to the refinement and depth of my work.

Additionally, I extend my sincere gratitude for the guidance and advice provided by the members of the review committee, Professor Dr. Kohei Nagai and Professor Dr. Takashi Matsumoto. Their thoughtful comments and encouraging remarks enriched my work from various perspectives and were instrumental in enhancing the quality of my research.

I am grateful to the current and former laboratory members for their help and support. Special appreciation goes to Ms. Naoko Masaki, our diligent secretary, for her continuous support, including managing financial matters related to research and assisting with personal challenges. Her efficiency and kindness made a significant difference during my time at the lab.

I would like to express my gratitude to my family and friends for their unwavering support. I thank my late father, Mr. Bennie Milandu Hamunzala, and my late mother, Mrs. Charity Handenda Chombe, whose memories continue to inspire me. I am also grateful to my uncle, Mr. Costen Chilala, Dr. Charles Kahanji, and my elder friend, Mr. Ignatius Choongo, for their encouragement and support, which motivated and inspired me to pursue higher education at Hokkaido University, Japan.

Special appreciation and thanks go to my wife, Namwase Mubagwe, for her unwavering support and encouragement throughout my doctoral program at Hokkaido University, Japan. Her resilience and strength, even in the face of challenges such as her breast cancer diagnosis on December 29, 2023, were inspiring and provided me with the courage to persevere. Her love and dedication have been a constant source of motivation, and I am profoundly grateful for her presence in my life. Namwase's unwavering faith in my abilities, her patience during my long hours of study and research, and her ability to maintain a positive outlook despite the adversities we faced together, have been truly remarkable. Her sacrifices and unwavering belief in the importance of my work have not only enabled me to complete this journey but have also enriched my life in ways I cannot fully express. Her strength and unwavering support have been the bedrock of my success, and for that, I am eternally grateful.

I sincerely thank Mulungushi University, Zambia, my current employer, for granting me study leave to pursue my doctoral studies at Hokkaido University, Japan. I am deeply grateful for this opportunity and the unwavering support provided by this institution. This journey would not have been possible without their encouragement and assistance.

I also extend my heartfelt thanks to the Road Development Agency, Zambia for their cooperation and assistance in granting me permission to collect data on road bridges in Zambia. I am deeply appreciative of their support, which was essential for the successful completion of this research.

Finally, I would like to thank the Japan International Cooperation Agency (JICA) for their financial support, road asset management seminars, Japanese modernization studies, and JICA social events throughout my tenure. Their assistance was invaluable, allowing me to focus on my research without financial worries. Additionally, their programs offered a broader perspective on international collaboration and development, enriched my social life and personal growth, and provided networking opportunities among JICA scholars, engineering experts in civil and bridge engineering, and university professors and researchers. This comprehensive support system greatly enhanced my academic and professional journey, fostering meaningful connections and expanding my knowledge and skills in the field.

To all who contributed to this journey, your support and encouragement have been invaluable, and I am profoundly grateful.

Bennie Hamunzala
Hokkaido University, 2024

Abstract

Effective management of bridge infrastructure is crucial for ensuring safety and longevity with limited resources. This study proposes an improved method for estimating construction years of road bridges using remote sensing and statistical analysis techniques. The use of bridge age and damage ratings is a cost-effective approach for evaluating the deterioration rates and predicting the future physical conditions of road bridges. Bridge authorities and organizations can benefit from this method, enabling them to prioritize maintenance and repairs effectively. The purpose of this study is to develop a clear and objective method for estimating construction years of road bridges, addressing the limitations of previous research.

The study aims to provide a reliable tool for bridge authorities and organizations to manage bridge infrastructure effectively. The method's accuracy and reliability are crucial for informing maintenance and repair decisions. The study utilizes the remote sensing data, the Normalized Difference Water Index 2 (NDWI_2), from Landsat 5 Thematic Mapper and Landsat 7 Enhanced Thematic Mapper Plus. Google Earth Engine (GEE) processes and analyzes the NDWI_2 data. The Sequential T-test Analysis of Regime Shift (STARS) method identifies the estimated construction year from the analyzed NDWI_2 data. The NDWI_2 is a function of near-infrared (NIR), and shortwave infrared 2 (SWIR2) bands, mathematically expressed as: NDWI_2 = (NIR - SWIR2) / (NIR + SWIR2).

The performance of the method was tested in Nago City, Japan, Cambodia, and Zambia. The results show promising accuracy, with correctly estimated construction years for road bridges in Nago City, Cambodia, and Zambia. The regression analysis yielded R^2 values of 0.33, 0.06, and 0.64 for the bridges in Nago City, Japan, Cambodia, and Zambia, respectively. The overall absolute mean errors determined were 2.69, 4.93, and 13.79 for the bridges in Nago City, Cambodia, and Zambia, respectively. The estimated number of correctly identified bridges with estimated construction years in Nago City were 39 out of 44 road bridges, 423 out of 649 road bridges in Cambodia, and 14 out of 27 in Zambia. The study's findings demonstrate the potential of remote sensing and statistical analysis techniques in accurately estimating the construction years of road bridges. The relatively low R^2 values may be attributed to insufficient reflectance due to atmospheric absorption and scattering effects. In addition, differences between the planned year of construction recorded in the database and the actual year of construction may have contributed to the discrepancy between the estimated construction years and actual construction years, resulting in lower R^2 values. Such discrepancies may have been caused by construction delays. The limited number of road bridges tested in Zambia was due to the insufficient availability of road bridge data with known years of construction.

The improved method offers significant time and cost savings, particularly for road bridges with unknown construction years. It also serves as a valuable planning tool for bridge maintenance and improvement. The methodology holds promise beyond road bridges, extending to the determination of construction years for other structures. The study's contributions include the development of an objective and clear method for estimating the construction years, the demonstration of the method's accuracy and reliability, and the potential for broader applications in infrastructure management.

The method's objectivity and clarity make it a valuable tool for bridge authorities and organizations. Future studies can build on this research to improve the accuracy and reliability of construction year estimates. The study's findings have implications for infrastructure management, highlighting the importance of accurate construction year estimates for effective maintenance and repair decisions.

Keywords: bridge infrastructure management, normalized difference water index 2, remote sensing analysis, estimated construction year of a road bridge, STARS method

Contents

List of Tables

List of Figures

Chapter 1

1 Introduction

1.1 Background

Effective management of bridge infrastructure is imperative to ensure safety, longevity, and sustainability amidst limited resources [1–4]. Bridges serve as critical components of transportation networks, facilitating the movement of goods and people across various regions. However, maintaining and managing these structures pose significant challenges for bridge authorities and organizations worldwide, mainly due to [5–11]:

- Inadequate budgets
- Shortage of qualified engineers
- Deficiencies in technological capabilities
- Severe environmental conditions
- Higher loads
- Aging bridge infrastructure

Inadequate funding is a primary challenge in bridge management. Many bridge authorities operate with constrained budgets that limit their ability to perform necessary maintenance and upgrades. Insufficient funding can result in deferred maintenance, which accelerates the deterioration of bridge components and can lead to structural failures [12].

The shortage of qualified bridge engineers further exacerbates the problem of managing bridge infrastructure effectively. Engineering professionals with specialized knowledge in bridge design, maintenance, and rehabilitation are in high demand but short supply [13].

Technological deficiencies also pose significant challenges to bridge management. Advanced technologies such as structural health monitoring systems, non-destructive testing methods, and data analytics are crucial for effective bridge maintenance [14].

Bridges are exposed to a variety of severe environmental conditions that can significantly impact their structural integrity [15]. Factors such as extreme temperatures, heavy rainfall, flooding, and seismic activity contribute to the deterioration of bridge materials and components.

Modern transportation demands have led to higher loads on bridges than those originally anticipated during their design and construction [16]. Managing these higher loads requires careful assessment and potential retrofitting of existing structures.

During the mid-20th century infrastructure booms, a substantial number of bridges were constructed to meet growing transportation needs. However, today, as these bridges approach or surpass their intended lifespans, they encounter significant challenges. These structures now require increased maintenance efforts and face heightened vulnerabilities due to natural wear and tear, material fatigue, the strain of heavier loads than originally anticipated, and exposure to harsh environmental conditions.

Addressing these issues requires a multifaceted approach involving:

- Increased funding for bridge maintenance and upgrades
- Investment in education and training programs for engineers
- Adoption of advanced and cost-effective technologies for bridge management
- Strategic planning to mitigate environmental impacts and accommodate modern transportation demands
- Development of sustainable and resilient bridge design practices
- Implementation of regular inspection and maintenance protocols
- Collaboration between bridge authorities, engineers, and researchers to share knowledge and best practices

Ensuring the safety, longevity, and sustainability of bridge infrastructure is crucial for maintaining effective transportation networks and supporting economic growth. By adopting a proactive and multidisciplinary approach, bridge authorities and organizations can overcome the challenges facing bridge management and provide safe and reliable transportation infrastructure for future generations.

1.2 Remote Sensing Techniques in Bridge Management

Remote sensing is the process of acquiring information about objects or areas from a distance, typically using sensors, and these sensors can be mounted on an aircraft, drone or satellites [17, 18]. The sensors detect and record electromagnetic radiation reflected or emitted from surfaces. Remote sensing is classified into two main types: active and passive. Active remote sensing involves emitting energy towards an object and analyzing the reflected energy, such as with RADAR or LiDAR systems [19]. Passive remote sensing, on the other hand, detects natural energy that is reflected or emitted from the observed scene, such as with optical or thermal sensor [21].

Both types of remote sensing have proven valuable in the field of bridge management, providing critical data for:

- Maintenance planning and scheduling
- Structural health monitoring
- Condition assessment and rating
- Damage detection and repair
- Bridge design and construction

The integration of remote sensing technology into bridge management practices enhances the efficiency and effectiveness of maintenance and monitoring activities, leading to improved safety, reduced costs, and extended bridge lifespan.

1.2.1 Active Remote Sensing in Bridge Management

Active remote sensing systems emit their own energy towards the target. This energy typically takes the form of electromagnetic radiation. Active remote sensing technologies have revolutionized bridge management, offering accurate and reliable data for informed decision-making [20]. Two prominent examples of active remote sensing technologies are:

- Light Detection and Ranging (LiDAR)
- Synthetic Aperture Radar (SAR)

LiDAR systems emit laser pulses and measure the time it takes for the pulses to return after striking an object, creating precise 3D models of bridge structures. This technology enables detailed assessments of bridge condition and geometry, facilitating:

- Accurate damage detection

- Precise structural monitoring
- In-depth condition assessment

Similarly, SAR uses radar signals to produce high-resolution images of bridges, useful for detecting:

- Structural deformations
- Displacements

One of the primary advantages of active remote sensing is its ability to operate under various weather conditions and during both day and night [22]. This capability ensures consistent data acquisition, crucial for monitoring the health of bridge structures over time [23]. Additionally, active remote sensing systems, like LiDAR, offer:

- High spatial resolution
- High accuracy

Making them suitable for detecting minute structural changes that could indicate potential issues [24, 25].

Despite its advantages, active remote sensing also has some limitations, including:

- High cost of high-resolution data
- Limited coverage
- Insufficient field validation data
- Specialized expertise required for data processing and analysis

These limitations highlight the need for careful consideration and strategic planning when implementing active remote sensing technologies in bridge management [22, 26].

1.2.2 Passive Remote Sensing in Bridge Management

Passive remote sensing relies on natural energy sources, primarily the sun, to gather data [18]. This category includes:

- Optical imagery
- Thermal infrared sensors

Optical imagery provides visual information about the surface condition of bridges, which can be used to:

- Identify visible defects such as cracks and corrosion
- Detect changes in bridge geometry and appearance

Thermal infrared sensors detect heat emitted by objects, which can be useful in:

- Identifying areas of thermal anomalies that may indicate structural weaknesses
- Detecting water leakage or moisture issues

Passive remote sensing technologies are generally less expensive compared to active systems. The availability of a wide range of satellite imagery, often at no cost, allows for extensive monitoring without significant financial investments. Additionally, passive sensors can cover large areas, providing comprehensive overviews of bridge networks, which is beneficial for:

- Large-scale monitoring and management
- Identifying potential issues before they become major problems

However, passive remote sensing also faces certain drawbacks. Its reliance on natural light means that data acquisition can be hindered by:

- Weather conditions, such as cloud cover

- Limited daylight hours

Furthermore, the spatial resolution of some passive sensors may not be sufficient to detect small-scale structural issues, which can limit their effectiveness in detailed bridge inspections. Despite these limitations, passive remote sensing remains a valuable tool in bridge management, offering cost-effective and wide-area monitoring capabilities.

1.2.3 Application of Remote Sensing Techniques and its Significance

Numerous studies have demonstrated the effectiveness of remote sensing in bridge management [27–32]. For example, previous studies have used remote sensing techniques with interferometric synthetic aperture radar (InSAR) and high-resolution satellites to extract features and monitor structural deformations of bridge infrastructures on the Earth's surface. With increasing traffic loads on bridges, challenging environmental conditions such as flooding, wind loads, and other factors, and limited capital investment for bridge maintenance, repair, and rehabilitation, InSAR techniques can complement visual inspections as a source of timely information regarding early signs of bridge infrastructure damage.

InSAR techniques offer several advantages, including:

- Day and night monitoring capabilities
- Ability to penetrate cloud cover
- Production of accurate and high-resolution imagery
- High-density measurements
- Relatively short satellite repetition time
- Cost-effective and near real-time method

However, processing the collected InSAR data is time-consuming and requires expertise.

In another study, researchers developed a method for estimating the construction year of road bridges using the Normalized Difference Water Index (NDWI) [34]. NDWI is a function of visible green and near-infrared (NIR) bands, mathematically expressed as:

$$\text{NDWI (Normalized Difference Water Index)} = \frac{\text{Visible Green} - \text{NIR}}{\text{Visible Green} + \text{NIR}} \tag{1}$$

NDWI is a tested and proven passive remote sensing technique used as an indicator of water resources [37]. The method utilized Landsat 5 Thematic Mapper and Landsat 7 Enhanced Thematic Mapper Plus to collect the visible green and near-infrared bands. The collected bands constitute the NDWI, which is analyzed in Google Earth Engine. The estimated construction year from the analyzed NDWI data was determined visually. However, the final results for the method of estimating the construction year of road bridges were unclear, and the technique for identifying the final year from the analyzed NDWI data was subjective.

Both active and passive remote sensing technologies offer significant advantages for the management of bridge infrastructure. They provide critical data that can help ensure the safety, longevity, and sustainability of bridges. The integration of remote sensing technologies in bridge management is of significant importance. These technologies enable regular and comprehensive monitoring of bridge conditions, which is essential for ensuring the safety and longevity of these structures. By detecting issues early, remote sensing can help prevent catastrophic failures, thereby protecting lives and reducing maintenance costs.

While the benefits of remote sensing in bridge management are clear, several challenges remain. The high cost of active remote sensing technologies and the need for specialized skills for data interpretation are significant barriers. Additionally, integrating remote sensing data with existing bridge management systems can be complex and time-consuming. Advancements in remote sensing technologies, such as the development of more affordable and user-friendly systems, could further enhance their application in bridge management. Increased collaboration between technology providers and bridge authorities could also facilitate the adoption of these technologies, improving the overall efficiency and effectiveness of bridge maintenance and monitoring.

1.2.4 Construction Years of Road Bridges in Bridge Management

The construction years of road bridges is a critical piece of information in bridge management [34]. It provides valuable insights into the bridge's age, design, and materials, which are essential for assessing its condition, predicting its remaining lifespan, and prioritizing maintenance and repair works [35]. Despite its significance, the construction year is often unknown or uncertain, particularly for older bridges, and small to medium road bridges. In this study, small to medium road bridges are typically defined as bridges with an overall length of 100 meters or less. The lack of information regarding the construction year of road bridges can result in inaccurate assessments and ineffective bridge management strategies.

Knowing the construction year of a road bridge is crucial in bridge management for several reasons:

- Age-related deterioration: Bridges deteriorate over time due to environmental and traffic-related factors. Knowing the construction year helps estimate the bridge's age and predict its remaining lifespan.
- Design and materials: The construction year provides information about the bridge's design and materials, which is essential for understanding its structural behavior and potential weaknesses.
- Maintenance and repair prioritization: Accurate knowledge of the construction year helps prioritize maintenance and repair works, ensuring that the most critical bridges receive attention first.
- Budgeting and planning: Knowing the construction year helps estimate the bridge's remaining lifespan, allowing for better budgeting and planning for future maintenance and replacement needs.

Several studies have utilized the construction year in bridge management:

- Sovisoth et al. [34] developed a method for estimating the construction year of road bridges using the Normalized Difference Water Index (NDWI).
- Kashiwa and Nagai [36] used the age and damage ratings of the road bridges to determine the deterioration rates of road bridges in Niigata Prefecture, Japan.

Let us delve deeper into the study by Kashiwa and Nagai [36]. The number of bridges analyzed in Niigata in Figure 1 was approximately 4000 road bridges [36]. The study utilized bridge age and damage ratings as key metrics. Damage age was determined by referencing the construction year of each road bridge, representing the elapsed years. The elapsed year is the difference between the year when the survey was conducted and the construction year of the road bridge. Conversely, damage ratings were derived from inspections carried out by bridge engineers during the same time period when the survey was conducted.

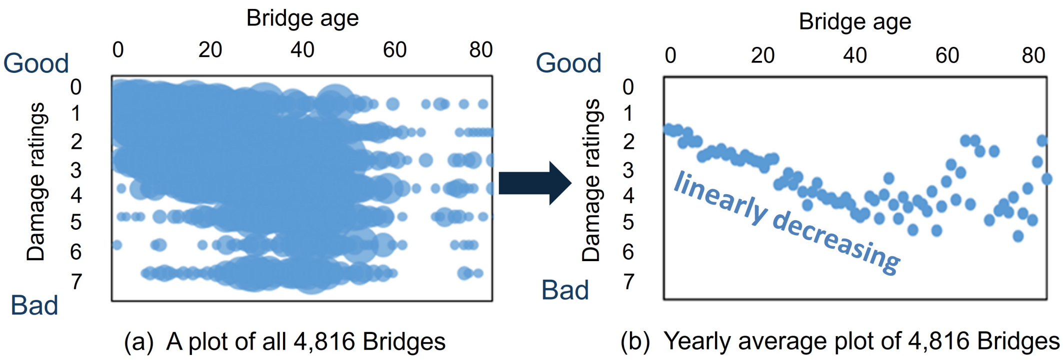

Figure 1: Damage estimation of Road Bridges in Niigata Prefecture, Japan

Figure 1(a) displays a cluster plot of approximately 4000 road bridges in Niigata Prefecture, showing no discernible trend. However, after computing the yearly average of the bridge age along the horizontal axis, the trend becomes evident, as illustrated in Figure 1(b). There is a linear decrease in trend up to 50 years, indicating an increase in the deterioration rate or a decrease in the soundness of road bridges within that timeframe. It's important to note that this analysis does not focus on the physical deterioration rate of individual bridges, but rather on the average physical deterioration rate of all bridges. This information is valuable for forecasting the future performance of bridges, as well as for budgeting, and scheduling bridge inspections and maintenance plans. After 50 years, the trend becomes less evident, with fewer data points available. The soundness values of bridges display a broad distribution beyond this timeframe. This variance results from the relatively small number of bridges aged over 50 years, with some undergoing repair and reconstruction. This phenomenon may be attributed to the implementation of damage recovery and repair work on many bridges once they reach the 50-year milestone.

These studies demonstrate the significance of the construction year in bridge management and highlight the need for accurate and reliable methods for estimating this information. Despite its importance, the construction year is often lacking for many bridges, especially small to medium bridges [34, 36]. This lack of information can lead to:

- Inaccurate assessments: Without knowing the construction year, bridge managers may rely on assumptions or rough estimates, leading to inaccurate assessments and ineffective management strategies.
- Inefficient maintenance: Bridges may receive unnecessary maintenance or repairs, wasting resources and potentially causing more harm than good.

- Safety risks: Unknown construction years can lead to unforeseen structural failures, posing safety risks to the public.

Efforts should be made to document and record the construction year of all bridges, especially small to medium bridges, to ensure accurate assessments and effective management strategies.

1.2.5 Problem Statement

The previous method [34], which estimates the construction year of road bridges using the Normalized Difference Water Index (NDWI), some limitations. The final result is not clear, and the process of identifying the construction year from the analyzed NDWI is subjective. The method employs three points on the bridge, each point located on an independent image pixel, as shown in Figure 2: one at the midspan of the road bridge and the other two positioned on each side perpendicular to the bridge, each at a distance of 35 meters. The previous method postulates that the NDWI of the three pixels are similar before the bridge is built. After the bridge is built, the NDWI of the target bridge point (TBP) shifts from that of the two reference pixels. The year in which the TBP shifts is considered the estimated year of construction.

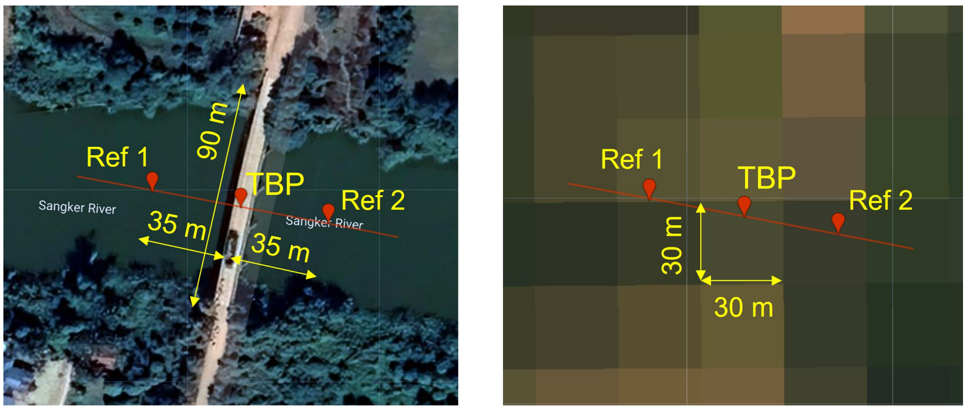

(a) Google Earth Engine image

(b) Pixelated satellite image for the year 2006

Figure 2: Chaeng Meanchey Road Bridge in Cambodia (Actual Construction Year: 2006)

The visible green and near-infrared bands in Landsat 5 Thematic Mapper and Landsat 7 Enhanced Thematic Mapper Plus were collected from each pixel; the target bridge point

(TBP), and two reference points (Ref. 1 and Ref. 2). NDWI is a function of visible green and near-infrared (NIR), mathematically expressed as: NDWI = (Visible Green - NIR)/(Visible Green + NIR).

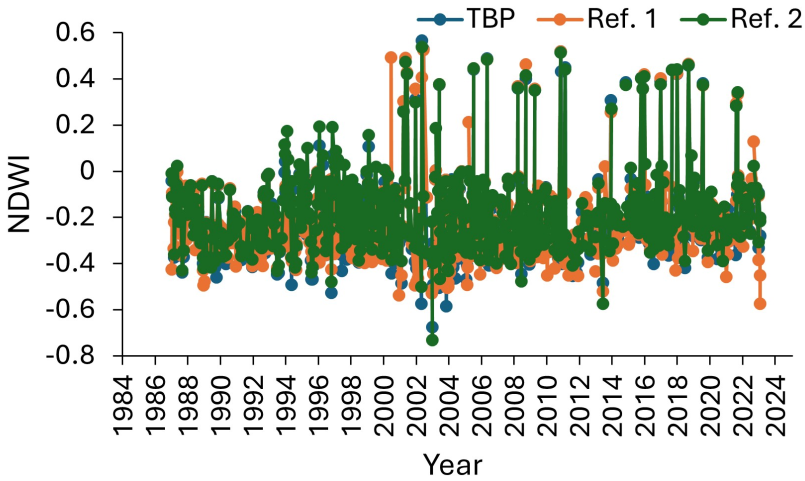

Figure 3: NDWI values for TBP, Ref. 1, and Ref. 2 over time for Chaeng Meanchey Road Bridge in Cambodia (Actutal Construction Year: 2006)

The TBP, Ref. 1 and 2 are analyzed in Google Earth Engine using the NDWI. The NDWI results of the TBP, Ref. 1, and Ref. 2 are plotted together on the same reference frame, as shown in Figure 3. Although the NDWI trends are not clearly visible in Figure 3, a closer examination reveals a subtle shift in the TBP's NDWI values compared to the reference points, indicating a potential shift in the NDWI. Further analysis is required to determine the significance of this shift and its relationship to the bridge construction.

1.2.6 Aim of the Study

The aim of this study is to improve the method in the previous study [34]. To address the limitations, we utilize the Normalized Difference Water Index 2 (NDWI_2), a function of near-infrared (NIR) and shortwave infrared 2 (SWIR2), mathematically expressed as: NDWI_2 = (NIR - SWIR2)/(NIR + SWIR2)

To enhance the accuracy of the method, we process the NDWI_2 data to reduce noise and annually average the data to minimize seasonal variations. Google Earth Engine is used for processing and annual averaging of the NDWI_2 data. Subsequently, we employ the Sequential T-test Analysis of Regime Shift (STARS) method to identify the estimated construction year from the analyzed NDWI_2 data.

The STARS method, introduced by Rodionov [39], is a robust statistical technique based on the two-sample t-test. It detects shifts in time series data by calculating the differences between consecutive mean values. In the context of this study, the improved method postulates that before the bridge is built, NDWI_2 values are relatively constant. However, immediately after the bridge is constructed, NDWI_2 values shift downwards. The year when this shift occurs is considered the estimated year of construction.

The improved method offers a clear and objective approach for estimating the construction year of road bridges. It provides a cost-effective technology for determining the deterioration rates of road bridges, assisting in bridge management.

1.2.7 Objectives of the Study

1. To develop a clear and objective method for estimating the construction years of the road bridges.
2. To identify a more accurate index for estimating the construction years of road bridges from the 12 indices.
3. To compare the performance of the previous method and the improved method.
4. To assess the improved method's accuracy in estimating the construction years of road bridges in:
   (a) Nago City, Japan, considering the region's unique environmental and infrastructure characteristics.
   (b) Cambodia, taking into account its effectiveness in different geographical settings.
   (c) Zambia, assessing its effectiveness across various regions.

The 12 indices attempted in this study are presented Table 1.

Table 1: The 12 Indices Attempted in this Study

Index	**Description**	**Application in Remote Sensing Studies**
NDVI	Normalized Difference Vegetation Index	For mapping vegetation
GNDVI	Green Normalized Difference Vegetation Index	↓
BNDVI	Blue Normalized Difference Vegetation Index	↓
NDWI_1	Normalized Difference Water Index 1	For mapping water bodies and moisture content in vegetation
NDWI_2	Normalized Difference Water Index 2	↓
NDWI_3	Normalized Difference Water Index 3	↓
NDWI_4	Normalized Difference Water Index 4	↓
NBR2	Normalized Burn Ratio 2	For mapping burnt areas
NDSI	Normalized Difference Soil Index	For mapping soils
DBSI	Dry Bare Soil Index	↓
NDBI	Normalized Difference Built-up Index	For mapping urban areas
BI	Built-up Index	↓

The indices in Table 1 are widely used in remote sensing applications and offer a comprehensive range of metrics for assessing various land cover features. By evaluating the performance of the indices in Table 1, this study aims to identify the most effective indices for estimating the construction year of bridges.

By achieving these objectives, this study will contribute to the development of more effective bridge management strategies, enhancing the safety and longevity of road bridges. The use of remote sensing technology will provide a cost-effective method for determining the deterioration rates of road bridges, assisting in prioritizing maintenance and repair works, and ensuring the sustainable management of infrastructure resources.

The construction year of road bridges is a critical piece of information in bridge management. Its significance extends beyond mere historical interest, as it provides valuable insights into the bridge's condition, design, and materials. Further research is needed to develop accurate and reliable methods for estimating the construction year, particularly for older bridges, and small to medium road bridges. Additionally, efforts should be made to document and record the construction year of all bridges to ensure accurate assessments and effective management strategies.

1.3 Outline of the Dissertation

This thesis is structured into five chapters, each addressing a specific aspect of the research.

Chapter 2 develops an improved method for estimating the construction years of road bridges using the Normalized Difference Water Index 2 (NDWI_2). This chapter also assesses the performance of 12 indices by estimating the construction years of only two road bridges, and evaluates the performance of NDWI_2 by applying the improved method to estimate the construction years of road bridges in Nago City, Japan.

Chapter 3 applies the improved method to estimate the construction years of road bridges in Cambodia and compares the performance of the improved and previous methods. This chapter provides a comprehensive evaluation of the improved method's accuracy and reliability.

Chapter 4 extends the application of the improved method to Zambia, exploring its performance in a diverse geographical and cultural context.

Chapter 5 presents the conclusions, recommendations, and significance of the research, summarizing the key findings and outlining potential avenues for future investigation.

Chapter 2

2 Development of the Improved Method and Application of the Improved Method in Nago City, Japan

2.1 Introduction

Road bridges are critical infrastructure assets that require regular maintenance and management to ensure public safety and transportation efficiency. Accurate knowledge of a bridge's age is essential for assessing its structural integrity and prioritizing maintenance and repair works. However, the lack of accurate records and limited access to historical data often hinder the estimation of road bridge construction years. This study addresses this knowledge gap by developing an improved method for estimating road bridge construction years.

This study aims to develop an improved method for estimating the construction year of road bridges with enhanced clarity and objectivity. Building upon the previous method proposed by Sovisoth et al. [34], the improved method addresses its limitations and offers a more robust solution. The improved method employs the remote sensing and statistical analysis techniques to provide accurate estimates of road bridge construction years. The effectiveness of twelve indices will be tested on two road bridges by estimating their construction years, and the performance of the improved method will be evaluated on forty-four road bridges in Nago City.

The improved method uses Landsat 5 Thematic Mapper (TM) and Landsat 7 Enhanced Thematic Mapper Plus (ETM+) to collect near-infrared and shortwave infrared bands. The Normalized Difference Water Index 2 (NDWI_2), a function of near-infrared and shortwave infrared bands, is processed in Google Earth Engine (GEE) to remove noise and annually averaged to reduce seasonal variations. The processed NDWI_2 is then analyzed in GEE, and the Sequential T-test Analysis of Regime Shift (STARS) method is used to identify the estimated year of construction.

The previous method [34] used Landsat 5 TM and Landsat 7 ETM+ to collect visible green and near-infrared bands. The Normalized Difference Water Index (NDWI), a function of visible green and near-infrared bands, was analyzed in Google Earth Engine (GEE). However, the method had two significant limitations: (1) the process for identifying the estimated construction year from the analyzed NDWI was subjective, and (2) the method lacked clarity in its approach.

This study demonstrates that the improved method, leveraging NDWI_2 and STARS method, provides a more accurate and objective estimation of road bridge construction years compared to the previous method.

The improved method has significant implications for infrastructure management, urban planning, and historical research. By providing accurate and reliable estimates of road bridge construction years, the method can inform maintenance and rehabilitation strategies, support urban planning decisions, and enrich historical research.

The following sections of this research will provide a detailed overview of the improved method, its applications, and its potential implications for various stakeholders. The study's findings will contribute to the development of innovative infrastructure management strategies, enhancing public safety and transportation efficiency.

2.2 Landsat Mission

The Landsat mission stands as the longest-running space-based record of the Earth's surface and atmosphere [43], as illustrated in Figure 4.

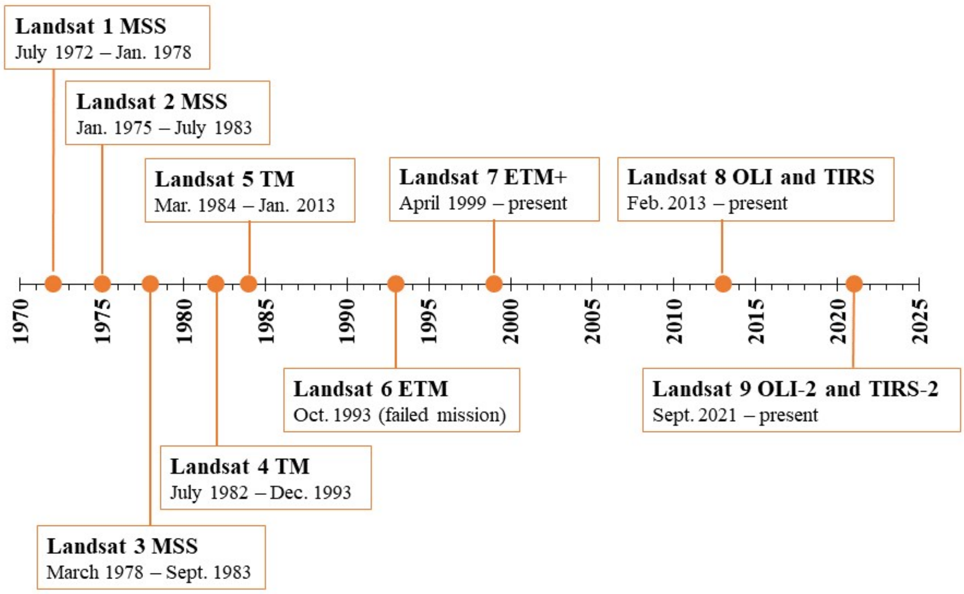

Figure 4: The Landsat mission commenced in 1972

It is managed jointly by the National Aeronautics and Space Administration (NASA) and the United States Geological Survey (USGS), and its primary objective is to monitor, manage, and comprehend the Earth's resources essential for supporting human life and other living organisms. The mission comprises eight operational Earth observation satellites, equipped with remote sensors to gather data and images of our planet. Additionally, one satellite mission, Landsat 6, encountered failure, as depicted in Figure 4.

The following sensors are mounted on the Landsat satellites: MSS—Multispectral Scanner System; TM—Thematic Mapper; ETM—Enhanced Thematic Mapper; ETM+—Enhanced Thematic Mapper Plus; OLI—Operational Imager, OLI-2—Operational Imager 2; TIRS—Thermal Infrared Sensor; and TIRS-2—Thermal Infrared Sensor 2.

This study employs Landsat 5 Thematic Mapper or both Landsat 5 Thematic Mapper and Landsat 7 Enhanced Thematic Mapper Plus for data analysis within the Google Earth Engine platform.

2.3 Spectral Bands and Indices

Spectral bands in remote sensing comprise segments of the electromagnetic spectrum ranging from visible light to optical and infrared radiation and microwave radiation. These spectral bands are used by various sensors to collect information about the Earth [44]. The Landsat 5 Thematic Mapper (TM) has three visible bands, three infrared bands and one thermal infrared band, and Landsat 7 Enhanced Thematic Mapper Plus (ETM+) has three visible bands, three infrared bands, one thermal infrared band and one panchromatic band,as shown in Table 2.

Table 2: Band characteristics for Landsat 5 Thematic Mapper (TM) and Landsat 7 Enhanced Thematic Mapper Plus (ETM+)

Band Type	**Landsat 5 TM Wavelength (μm)**	**Landsat 7 ETM+ Wavelength (μm)**
Band 1—Visible Blue	0.45–0.52	0.45–0.52
Band 2—Visible Green	0.52–0.60	0.52–0.60
Band 3—Visible Red	0.63–0.69	0.63–0.69
Band 4—NIR	0.76–0.90	0.77–0.90
Band 5—SWIR1	1.55–1.75	1.55–1.75
Band 6—Thermal Infrared	10.40–12.50	10.40–12.50
Band 7—SWIR2	2.08–2.35	2.08–2.35

Continued on next page

Table 2: (continued from the previous page)

Band Type	**Landsat 5 TM Wavelength (μm)**	**Landsat 7 ETM+ Wavelength (μm)**
Band 8—Panchromatic	–	0.52–0.90

Note that the abbreviations in Table 2 are: NIR—short infrared; SWIR1—shortwave infrared 1; and SWIR2—shortwave infrared 2. The spatial resolution is 30 m for bands 1 through 5 and 7 for both Landsat 5 and Landsat 7. 120 m for band 6 in Landsat 5 and 60 m for band 6 in Landsat 7. 15 m for band 8 in Landsat 7.

A spectral index in remote sensing utilizes two or more spectral bands of an image per pixel, as outlined in Equations (2)–(13). These indices serve to enhance the observation of Earth's features like vegetation, water bodies, soil, and the urban areas. They enable the differentiation of features within an image and facilitate the modeling, prediction, or inference of surface processes [45].

$$\text{NDVI (Normalized Difference Vegetation Index)} = \frac{\text{NIR} - \text{Visible Red}}{\text{NIR} + \text{Visible Red}} \tag{2}$$

$$\text{GNDVI (Green Normalized Difference Vegetation Index)} = \frac{\text{NIR} - \text{Visible Green}}{\text{NIR} + \text{Visible Green}} \tag{3}$$

$$\text{BNDVI (Blue Normalized Difference Vegetation Index)} = \frac{\text{NIR} - \text{Visible Blue}}{\text{NIR} + \text{Visible Blue}} \tag{4}$$

$$\text{NDWI\_1 (Normalized Difference Water Index 1)} = \frac{\text{NIR} - \text{SWIR1}}{\text{NIR} + \text{SWIR1}} \tag{5}$$

$$\text{NDWI\_2 (Normalized Difference Water Index 2)} = \frac{\text{NIR} - \text{SWIR2}}{\text{NIR} + \text{SWIR2}} \tag{6}$$

$$\text{NDWI\_3 (Normalized Difference Water Index 3)} = \frac{\text{Visible Green} - \text{SWIR2}}{\text{Visible Green} + \text{SWIR2}} \tag{7}$$

$$\text{NDWI\_4 (Normalized Difference Water Index 4)} = \frac{\text{Visible Green} - \text{SWIR1}}{\text{Visible Green} + \text{SWIR1}} \tag{8}$$

$$\text{NBR\_2 (Normalized Burn Ratio 2)} = \frac{\text{SWIR1} - \text{SWIR2}}{\text{SWIR1} + \text{SWIR2}} \tag{9}$$

$$\text{NDSI (Normalized Difference Soil Index)} = \frac{\text{SWIR2} - \text{Visible Green}}{\text{SWIR2} + \text{Visible Green}} \tag{10}$$

$$\text{DBSI (Dry Bare-Soil Index)} = \frac{\text{SWIR1} - \text{Visible Green}}{\text{SWIR1} + \text{Visible Green}} - \text{NDVI} \tag{11}$$

$$\text{NDBI (Normalized Difference Built-up Index)} = \frac{\text{SWIR1} - \text{NIR}}{\text{SWIR1} + \text{NIR}} \tag{12}$$

$$\text{BI (Built-up Index)} = \frac{\text{SWIR1} - \text{NIR}}{\text{SWIR1} + \text{NIR}} - \text{NDVI} \tag{13}$$

The index described in Equation (2) represents one of the earliest studies on the application of the Normalized Difference Vegetation Index (NDVI). This research utilized Landsat 1 data to observe and quantify vegetation conditions across extensive areas [46]. Additional uses of NDVI include the estimation of crop yields, dry biomass, and alterations in surface conditions [47]. Equation (3) introduces another indicator of vegetation conditions known as the Green Normalized Difference Vegetation Index (GNDVI). Unlike NDVI, GNDVI is more sensitive to chlorophyll. By configuring the spectral bands in GNDVI as (green − NIR)/(green + NIR), a distinct index is derived, known as the Normalized Difference Water Index (NDWI), which serves as a marker for water resources [37].

Equation (4) presents an index analogous to NDVI and GNDVI. However, its utility is hampered by the susceptibility of the blue band to atmospheric interference, owing to its shorter wavelength and consequent heightened scattering effects [48]. Conversely, Equation (5) depicts an index adept at delineating liquid water within vegetation, exhibiting lesser susceptibility to scattering effects compared to NDVI [49]. Equation (6) presents an index proficient in depicting the water dynamics of seasonal wetlands [38]. Although Equation (7) serves as an indicator of open water bodies [50], however, it is surpassed by NDWI_4 [51] denoted as Equation (8).

The index in Equation (8) from [51] effectively identifies open water features while mitigating noise from vegetation, soil, and built environments, surpassing the NDWI from [37]. Additionally, it acts as an indicator of snow cover, also referred to as the Normalized Difference Snow Index [52]. Equation (9) presents an index indicative of burned areas and their severity [53], while Equation (10) enhances soil information [54]. Equation (11) maps built-up and bare areas in arid climates [55], whereas Equation (12) delineates urban built-up areas and, in certain instances, barren, wooded, and agricultural areas [56]. Finally, the index in Equation (13) exclusively maps built-up and barren areas [57].

2.4 Cloud Masking and Cloud Shadow Masking

Cloud masking and cloud shadow masking are filtering techniques used in remote sensing to eliminate pixels contaminated with clouds and cloud shadows. In cloud masking, the difference between the reflectance of clear images and that of cloud-contaminated images is used to recognize clouds. Conversely, cloud shadow masking relies on the difference in reflectance between clear images and those affected by cloud shadows to detect the latter. Both cloud masking and cloud shadow masking are used to reduce errors due to inaccurate mapping, increase visibility and consequently improve the reflectivity of the Earth's surface and the objects on it [58, 59]. In the current study, a computer code in

Google Earth Engine was used to perform the overall analysis including cloud masking and cloud cover reduction.

2.5 Sequential T-test Analysis of Regime Shift (STARS) Method

Sequential t-test analysis of regime shift (STARS) is a statistical method for detecting change points in time series data [39, 60, 61, 63]. The method identifies the point in time when the mean of the time series data changes significantly. The change in the mean can be either a single change or multiple changes within a time series. The STARS method is based on the statistical technique of the Student's t-test, and Rodionov [39, 60] describes the algorithm. The algorithm is coded in Visual Basic for use in a Microsoft Excel add-in and is available for download as freeware at `www.BeringClimate.noaa.gov`. The STARS method can be set to detect regimes with specific time scales and magnitudes. The inputs to the STARS Microsoft Excel add-in are the cutoff length l, the significance level α, and the Huber weight parameter H. The cutoff length l, and the significance level α are the main inputs that affect the magnitude of the regime shifts [62].

$$diff = |\bar{x}_{\text{new}} - \bar{x}_{\text{cur}}| = t\sqrt{\frac{2\sigma_l^2}{l}} \tag{14}$$

$$dof = 2l - 2 \tag{15}$$

$$t = t(\alpha, dof) \tag{16}$$

$$\bar{x}_{\text{crit}}^{\uparrow} = \bar{x}_{\text{cur}} + diff \tag{17}$$

$$\bar{x}_{\text{crit}}^{\downarrow} = \bar{x}_{\text{cur}} - diff \tag{18}$$

$$RSI = \frac{1}{l\sigma_l} \sum_{i=t_{\text{cur}}}^{m} (x_i - \bar{x}_{\text{crit}}), \quad m = t_{\text{cur}} + 1, \ldots, t_{\text{cur}} + l - 1 \tag{19}$$

The STARS method utilizes Equations (14)–(19) to analyze and determine the regime shift of the mean in the time series data. Equation (14) calculates the absolute difference, termed *diff*, between the mean values of the current regime, $\bar{x}_{\text{cur}}$, and the new regime, $\bar{x}_{\text{new}}$. Equation (15) represents the degree of freedom, *dof*, which is a function of the cutoff length, l. Equation (16) represents the t value from the t distribution, a function of the significance level, α and the degree of freedom, *dof* in Equation (15). The variance, σ_l^2, at any given l, is presumed constant, averaging over l-year intervals in the time series

x_i. Hence, *diff* remains constant throughout the session of x_i for each l value. At the current time t_{cur}, the mean value of the new regime ($\bar{x}_{\text{new}}$) is uncertain. However, it is anticipated to be equal to or greater than the critical level $\bar{x}^{\uparrow}_{\text{crit}}$ in the case of an upward shift, or equal to or less than $\bar{x}^{\downarrow}_{\text{crit}}$ for a downward shift, computed by Equation (17) and Equation (18), respectively. Equation (19) represents the regime shift index, *RSI*, which is a cumulative sum of the normalized anomalies relative to the critical level $\bar{x}_{\text{crit}}$.

In the current study, the STARS method was used to interpret the estimated construction year from NDWI_2 for both techniques. The inputs, cutoff length $l = 2$ to $l = \text{N}$, where N is the number of data points in the NDWI_2 dataset, significance level $\alpha = 0.05$, and Huber's weight parameter $H = 1$ were used. The cutoff length $l = 1$ can not be used, because it has no value of t in the t-distribution. Given that the cutoff length $l = 1$, $dof = 2l - 2 = 2(1) - 2 = 0$. From the cutoff length $l = 2$ to $l = \text{N}$, the optimal absolute maximum regime shift index *RSI* was determined and thus used to identify the estimated construction year.

2.6 Flowchart of the improved method

The method consists of four major steps, as outlined in Figure 5.

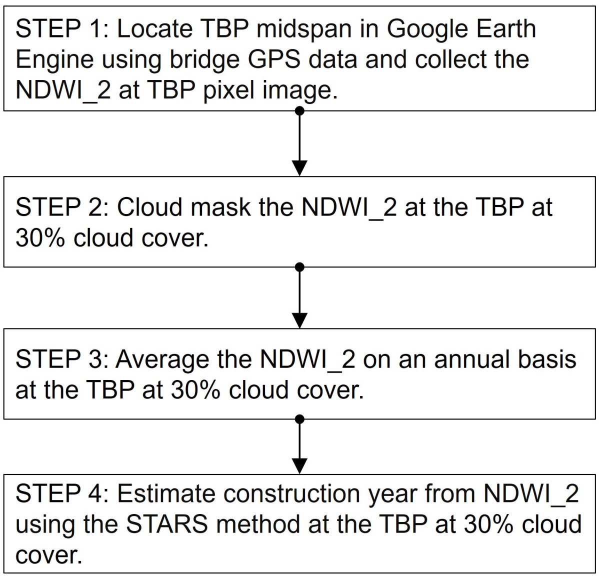

Figure 5: Method flowchart for the current study

In Step 1, the target bridge point (TBP) was located at the midspan of the road bridge using global positioning coordinates. The Normalized Difference Water Index 2 (NDWI_2) was collected from the pixel at the midspan of the road bridge. The collected data contained some noise.

In Step 2, the collected data was processed to remove the noise using cloud masking and cloud cover reduction techniques. Cloud masking filtered out pixels contaminated by clouds and cloud shadows, while cloud cover reduction excluded images with a cloud cover above a certain threshold. Both techniques reduced noise in the data and enhanced visibility. In this study, cloud cover was reduced to 30%.

In Step 3, the NDWI_2 cloud-masked data at 30% cloud cover at the TBP, were averaged annually. This procedure mitigated seasonal variations.

In Step 4, the Sequential T-test Analysis of Regime Shift (STARS) was applied to estimate the construction years of the road bridges. The STARS method was used on the NDWI_2 cloud-masked data at 30% cloud cover at the TBP. Results with p-values less than 0.05 were considered reliable.

2.7 An Example of Estimating the Construction Year of the Road Bridge

The data in Table 3 from the bridge database was used as an example in estimating the construction year of the bridge using this proposed technique.

Table 3: Characteristics of Chaeng Meanchey Road Bridge from the Bridge database

Bridge Name	**Country**	**Overall Length (m)**	**X-Coordinate**	**Y-Coordinate**	**Actual Construction Year**
Chaeng Meanchey	Cambodia	90	103.0753052	12.84854583	2006

2.7.1 Step 1: Locate the Mispan of the Target Bridge Point (TBP)

Using the coordinates from the bridge database system provided in Table 3, the midspan of the road bridge was located in Google Earth Engine (GEE). The newly generated coordinates at the midspan of the road bridge are presented in Table 4.

Table 4: Updated coordinates of Chaeng Meanchey Road Bridge at the midspan

Bridge Name	**Overall Length (m)**	**X-Coordinate**	**Y-Coordinate**	**Actual Construction Year**
Chaeng Meanchey	90	103.0752951992506	12.848565201269382	2006

The Google Earth image and the satellite pixelated image of the TBP at the midspan of the road bridge are shown in Figure 6. The reflectance values, represented as bands, were collected from the pixel at the TBP shown in Figure 6(b). The bands consist of visible blue, visible green, visible red, near-infrared, shortwave infrared 1, and shortwave infrared 2. These bands are used to constitute indices such as the Normalized Difference Water Index 2, which is a function of near-infrared and shortwave infrared 2 (NDWI_2). The index that was collected and used in this study is NDWI_2.

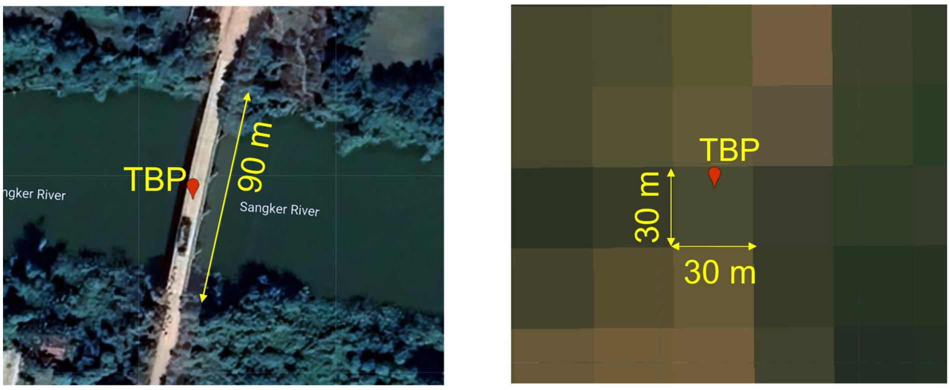

(a) Google Earth Engine image

(b) Pixelated satellite image for the year 2006

Figure 6: The midspan of Chaeng Meanchey Road Bridge

The NDWI_2 data collected at the midspan of the TBP has some instances of noise, as shown in Figure 7. The removal of this noise was done in Step 2 of the analysis. Figure 7 contains 589 data points spanning from 1984 to 2024. The NDWI_2 data at the midspan of the TBP was collected by merging images from Landsat 5 Thematic Mapper and Landsat 7 Enhanced Thematic Mapper Plus in Google Earth Engine.

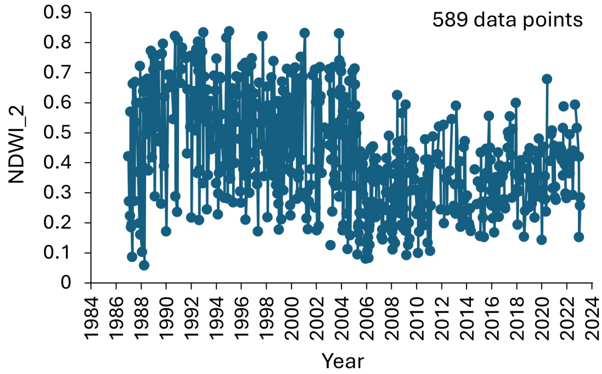

Figure 7: NDWI_2 with some noise data at the TBP

2.7.2 Step 2: Cloud Mask the NDWI_2 at the TBP at 30% Cloud Cover

In Step 2, the cleaning of noise data from the NDWI_2 was carried out in Google Earth Engine by using cloud masking and cloud cover reduction techniques. Both cloud masking and cloud cover reduction were applied to the data depicted in Figure 7, with the outcome displayed in Figure 8. The resulting dataset in Figure 8 comprises 230 data points spanning the years 1984 to 2024. The cloud cover in Figure 8 was reduced to 30%.

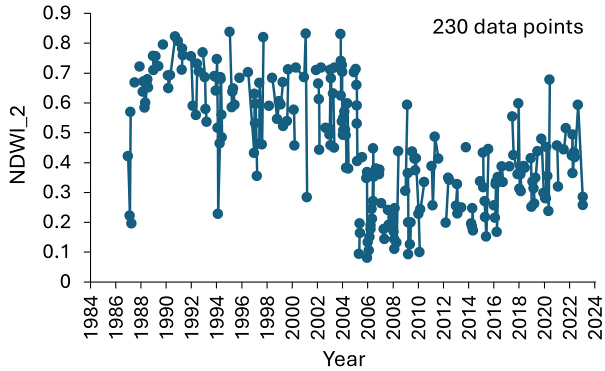

Figure 8: Cloud mask and cloud cover reduction of the NDWI_2 at the TBP

2.7.3 Step 3: Annually Average the NDWI_2 at the TBP at 30% Cloud Cover

In Step 3, annual averaging of the NDWI_2 at the TBP with 30% cloud cover in Figure 8 was performed to reduce the seasonal variations, yielding the outcome illustrated in Figure 9, whose trend was clear.

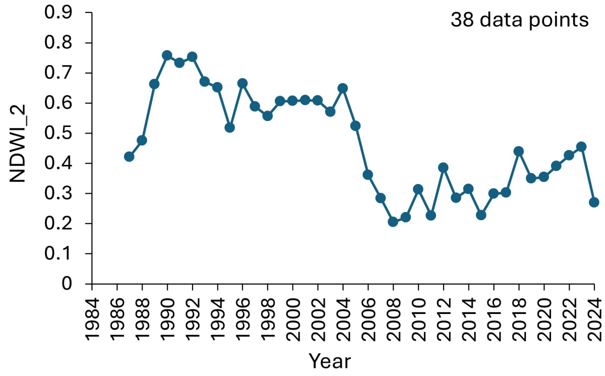

Figure 9: Annually average the NDWI_2 at the TBP

This process involved calculating the yearly average of NDWI_2 spanning the period from 1984 to 2024. The number of data points decreased from 230 in Figure 8 to 38 in Figure 9.

2.7.4 Step 4: Estimate Construction Year from NDWI_2 using the STARS Method at the TBP at 30% Cloud Cover

In Step 4, the Sequential T-test Analysis of Regime Shift (STARS) method was applied to the NDWI_2 in Figure 9, and the results shown in Figure 10 were generated. In Figure 10(a), the cutoff length l represents the sample size of the data analyzed, ranging from $l = 2$ to $l = 38$, because 38 data points are present in Figure 9. The Regime Shift Index (RSI) verifies that a shift has occurred. If the RSI is negative, a downward shift is indicated; otherwise, an upward shift is indicated if the RSI is positive.

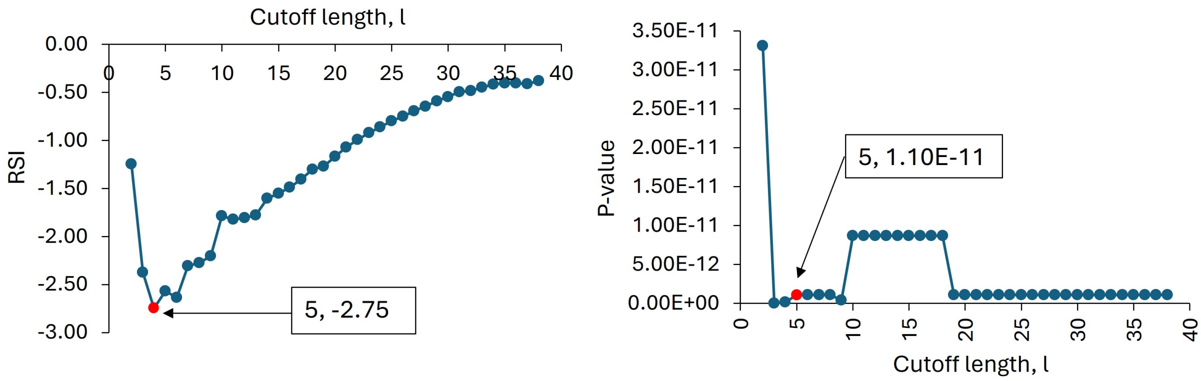

(a) The optimal regime shift index for the TBP

(b) The p-value for the TBP

Figure 10: Rgime shift index and p-value from the STARS method

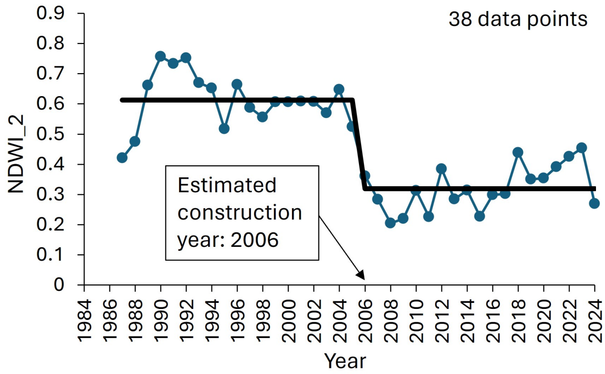

Figure 11: Estimated construction year from the STARS method for the TBP

In this study, a negative RSI was used. In Figure 10(b), the plot of the p-value against the cutoff length is shown. The optimal RSI was observed at $l = 5$, as depicted in Figure 10(a), with a p-value less than 0.05, as shown in Figure 10(b). The optimal RSI was applied again in the STARS method to generate the final plot in Figure 11, which estimates the construction year of the road bridge. The estimated construction year is 2006, which matches the actual construction year of 2006.

2.8 Road Bridges in Nago City, Japan

The study analyzed 44 road bridges in Nago City, Okinawa Prefecture, Japan, due to its diverse landscapes, making it an ideal testing ground for the proposed technique, as depicted in Figure 12. Nago City's climate is subtropical oceanic, with hot summers and mild winters [40]. Alongside Nago City, there are 8 major cities and 3 villages, also illustrated in Figure 12. Nago City's population is 63,554, covering 211 square kilometers [41]. It has 330 road bridges, selected from about 700,000 nationwide [42].

The 44 road bridges were chosen based on construction year (1990-2006) and overall length ($\leq$ 100 meters). The characteristics of the 44 road bridges in Nago City, classified by the overall length, road width, and year of construction, are shown in Table 5.

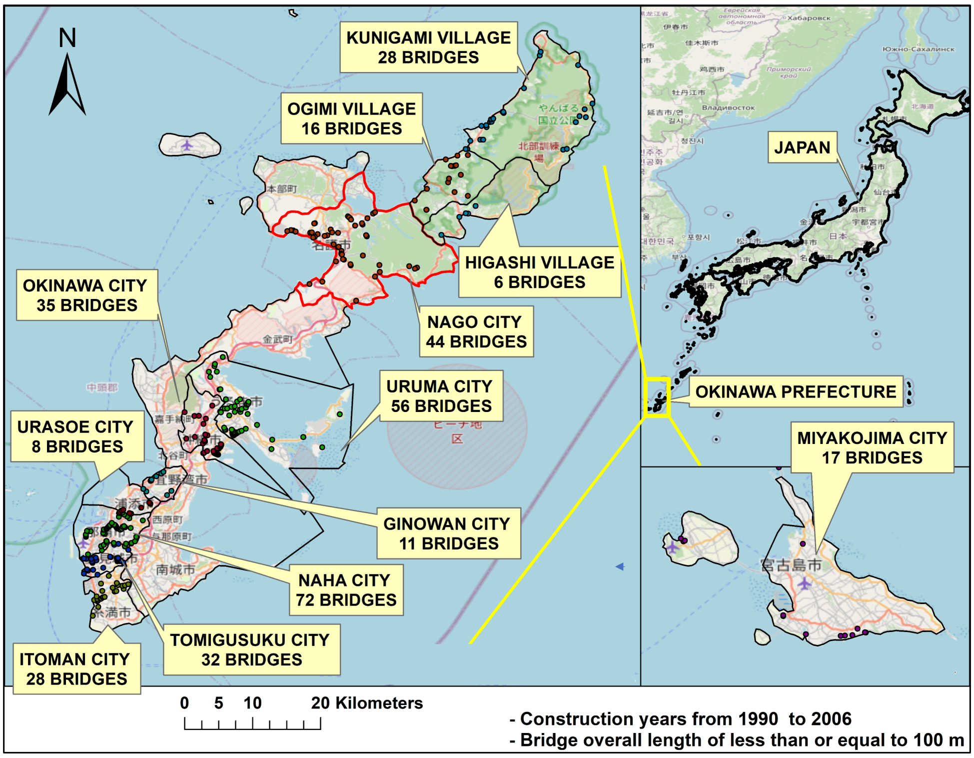

Figure 12: Road Bridges built in Nago City (1990-2006) with overall length of ≤ 100 meters, and surrounding major Cities and Villages in Okinawa Prefecture

Table 5: Characteristics of the 44 Road Bridges in Nago, City

Bridge Name	**Overall Length (m)**	**Width (m)**	**Surface Cover Type**	**Actual Construction Year**
Maeda	98.3	11.6	Forest	2006
Kuroyama	98.0	8.3	Forest	1997
Nagasaka	96.0	11.0	Forest	2000
Higashi Ebara	82.0	11.0	Forest	2003
Osuji	64.0	12.0	Forest	1992
Mijimai	56.7	7.0	Forest	1994
Higashiri	51.0	11.2	Forest	1997
Daikan	43.0	13.3	Forest	1992
Nagamata	42.0	11.5	Forest	1998
Kamifukuchi	37.0	11.5	Forest	1992
Makiya No.3	24.2	16.8	Forest	1991
Kamiyama	23.0	11.0	Forest	1993
Fukushi	21.8	5.0	Forest	1992
Second Geya	9.5	4.0	Forest	1996
Kamiyamatogawa	11.0	14.8	Forest	1992
Shitayamatogawa	11.0	14.8	Forest	1992
Blacksmith	33.9	6.5	Cropland	1992
Gabusoka	32.4	12.8	Cropland	1996
Haishi	27.9	12.5	Cropland	2002
Inada	30.6	5.5	Cropland	2003
Fukumi	70.0	11.0	Cropland	1992
Hane 105-2	31.0	6.0	Cropland	1993
Kayang Mata	22.3	5.0	Cropland	2001
Oura	77.0	15.8	Built-Up	1996
Higashi Yabu	56.6	17.1	Built-Up	2000
Furushima	47.0	16.0	Built-Up	1999
Nazaki	44.6	8.0	Built-Up	1994
Nakaoji	33.3	16.2	Built-Up	1993
Yonagawa	31.5	22.5	Built-Up	1992
Makiya No 2	28.3	18.8	Built-Up	1991
Kado River	25.0	22.5	Built-Up	1993
Tamemata	23.5	15.3	Built-Up	1990
Anwa Minamizaki	21.5	22.5	Built-Up	1991
Ose	44.0	5.0	Built-Up	1993
Name 162-1	18.2	4.0	Built-Up	1994

Continued on next page

Table 5 – continued from previous page

Bridge Name	**Overall Length (m)**	**Width (m)**	**Surface Cover Type**	**Actual Construction Year**
Sugita	25.0	15.6	Built-Up	1999
Hanejioo	24.6	7.5	Built-Up	1990
Maehira	23.1	6.6	Built-Up	1992
Yabu	46.5	14.3	Built-Up	1991
Anada	15.9	22.0	Built-Up	1992
Apanuku	11.8	4.0	Built-Up	1996
Lower River	16.0	7.0	Built-Up	1993
Makiya No. 1	11.8	20.1	Built-Up	1991
Minato	11.5	15.7	Built-Up	2000

2.9 Data collection and analysis

The United States Geological Survey (USGS) produces Landsat data in three tiers for each satellite: Tier 1, Tier 2, and Real-Time (RT) [64]. Tier 1 data meet geometric and radiometric quality requirements; Tier 2 data do not meet Tier 1 quality standards; and RT data have not yet been assessed. Based on quality and other factors, the collected data are classified into Collection 1—Level 1, Collection 1—Level 2, Collection 2—Level 1, and Collection 2—Level 2 [64,65]. The data are then processed into raw or digital numbers (DNs), top of atmosphere (ToA), and surface reflectance (SR). DN represent scaled and calibrated sensor radiance, ToA represents calibrated reflectance, and SR represents atmospheric-corrected reflectance.

2.9.1 Analysis of 12 Indices at Kuroyama and Kamiyama Road Bridges

The 12 indices in Equations (2)–(13) were analyzed at the target bridge point (TBP) using the method in Section 2.6 to understand their trends. Two road bridges, the Kuroyama road bridge and Kamiyama road bridge in Table 5, were analyzed using these indices at the TBP.

2.9.2 Analysis of NDWI_2 at 44 Road Bridges

The 44 road bridges in Table 5 were analyzed using the method in Section 2.6. The Normalized Difference Water Index 2 (NDWI_2) in Equations (6) was used at the target bridge point in the analysis.

2.9.3 Comparative Analysis of Current and Previous Method at Chaeng Meanchey Road Bridge

The Chaeng Meanchey road bridge in Figure 6 was analyzed and compared using both the previous and improved methods, with the improved method described in Section 2.6. The previous method postulates that the NDWI of the three pixels are similar before the bridge is built. After the bridge is built, the NDWI of the target bridge point (TBP) shifts from that of the two reference pixels. The year in which the TBP shifts is considered the estimated year of construction. The improved method postulates that before the bridge is built, the Normalized Difference Water Index 2 (NDWI_2) values are relatively constant. However, immediately after the bridge is constructed, NDWI 2 values shift downwards. The year when this shift occurs is considered the estimated year of construction. The mathematical expressions for NDWI and NDWI_2 are presented in Equations (1) and (6), respectively.

2.10 Results and Discussion

2.10.1 12 Indices at Kuroyama and Kamiyama Road Bridges

The 12 indices are presented in Equations (2)–(13). Two road bridges, Kuroyama road bridge and Kamiyama road bridge, were analyzed using the 12 indices at the target bridge point (TBP). The trends were clear and the estimated construction years for Kuroyama road bridge and Kamiyama road bridge were objectively determined using the Sequential T-test Analysis of Regime Shift, as shown in Figures 13 and 14, respectively.

All 12 indices were reasonably capable of estimating the construction years for both road bridges. The Normalized Difference Vegetation Index (NDVI), Normalized Difference Water Index 2 (NDWI_2), Blue Normalized Difference Vegetation Index (BNDVI), and Built-up Index (BI) recorded relatively high absolute mean differences.

The absolute errors between the actual and estimated construction years ranged from 0 to 5 years, with a p-value less than 0.05 for all 12 indices at both road bridges. This indicates that the results were accurate and statistically significant. However, no results were recorded for the Normalized Difference Water Index 3 (NDWI_3) and the Normalized Difference Soil Index (NDSI), as shown in Figures 14f and 14i for Kamiyama road bridge. This may be due to inadequate reflectance at Kamiyama road bridge and the fact that the two indices (NDWI_3 and NDSI) are both functions of visible green and shortwave infrared 2, with their numerator algebraic expressions arranged in opposite directions.

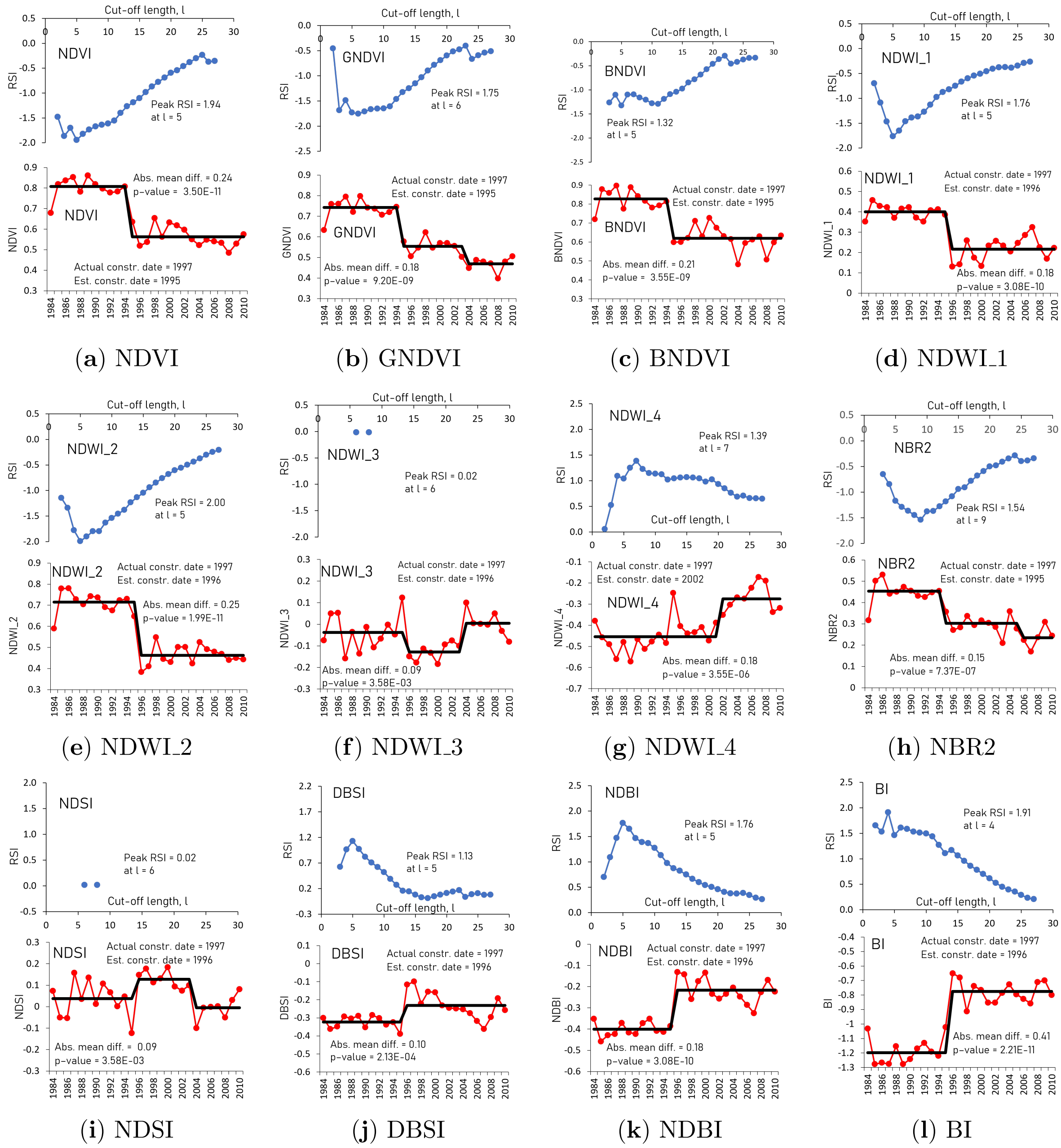

(**a**) NDVI (**b**) GNDVI (**c**) BNDVI (**d**) NDWI_1

(**e**) NDWI_2 (**f**) NDWI_3 (**g**) NDWI_4 (**h**) NBR2

(**i**) NDSI (**j**) DBSI (**k**) NDBI (**l**) BI

Figure 13: Kuroyama Road Bridge trends and results using the 12 indices

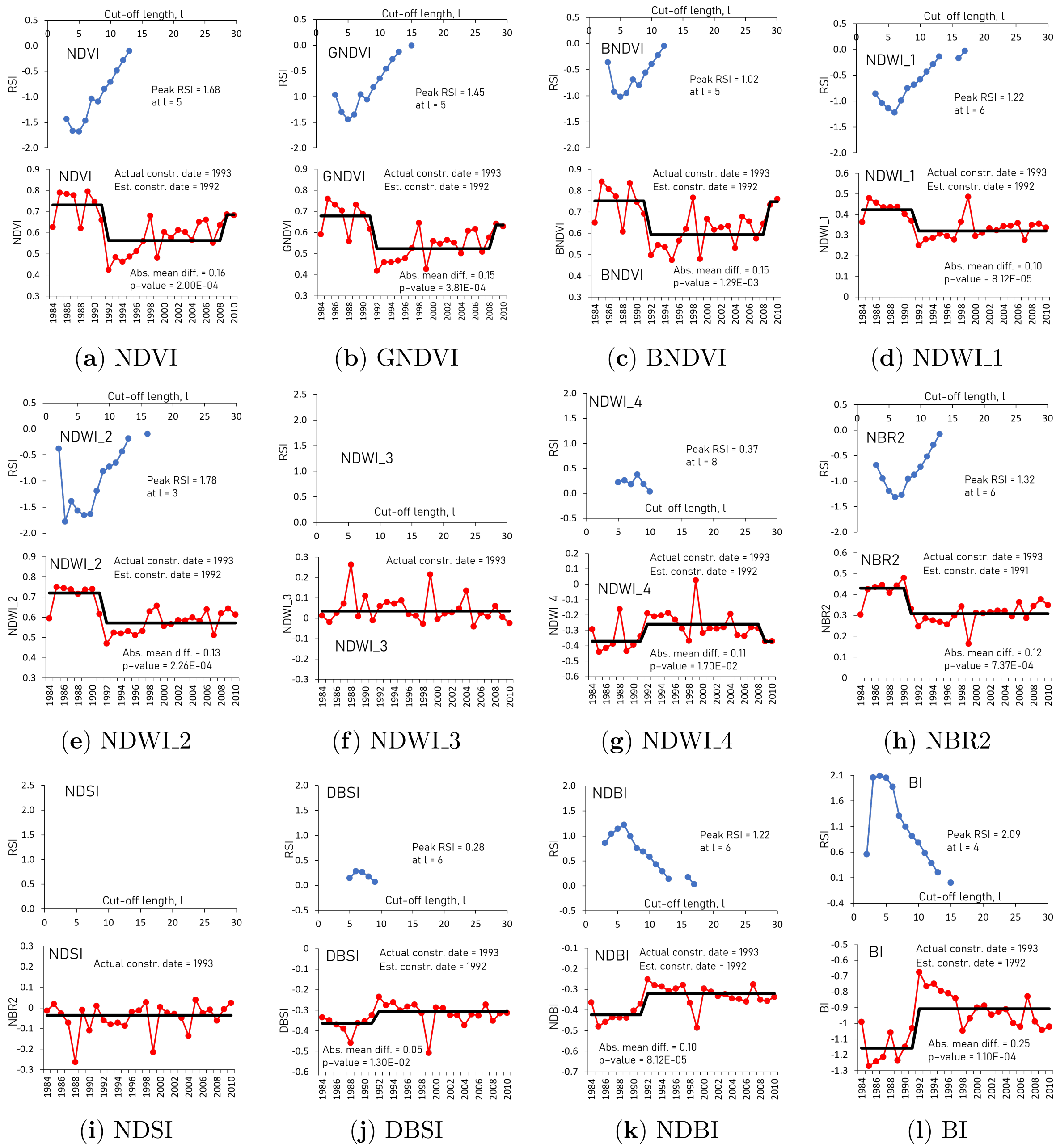

(a) NDVI (b) GNDVI (c) BNDVI (d) NDWI_1

(e) NDWI_2 (f) NDWI_3 (g) NDWI_4 (h) NBR2

(i) NDSI (j) DBSI (k) NDBI (l) BI

Figure 14: Kamiyama Road Bridge trends and results using the 12 indices

2.10.2 NDWI_2 at 44 Road Bridges

The Normalized Difference Water Index 2 (NDWI_2), as shown in Equations (6), was used for the analysis of 44 road bridges listed in Table 5. The estimated years of construction and p-values for these Bridges are shown in Table 6. The results of the regression analysis are presented in Figure 15 and the errors, which are the differences between the actual and estimated years of construction, are presented in Figure 16.

Figure 15 recorded a low R^2 value of 0.33 and an overall absolute error of 2.69 years. The method estimated the years of construction of 39 out of 44 road bridges, as shown in Table 6 and Figure 15. Of the 39 road bridges, 38 had a p-value of less than 0.05 and one bridge, Yabu road bridge, had a p-value of more than 0.05, as shown in Table 6. About 80% of the 44 road bridges had an absolute error in the range of 0 to 5 years, as shown in Figure 16. Three outliers were recorded in Figure 15, namely the Fukumi, Kayang Mata, and Sugita road bridges and five road bridges, namely Kamiyamatogawa, Shitayamatogawa, Lower River, Makiya No. 1 and Minato recorded no results, as shown in Table 6.

One of the possible explanations for the low R^2 value indicated by the gap between the actual and estimated year of construction in Figure 16 is that the planned year of construction recorded in the database may not correspond to the actual year of construction due to construction delays [34]. The overall absolute mean error of 2.69 years and p-value < 0.05 indicates that the results were accurate and statistically significant. According to the results in Figure 16, the histogram of errors follows a normal distribution, which may indicate that the predictions of the model are likely to be accurate and reliable. The inaccurate results for three road bridges and the lack of results for the five road bridges could be due to seasonal variations and inadequate reflectance.

Table 6: Estimated construction years and p-values of the 44 Road Bridges in Nago, City

Bridge Name	**Overall Length (m)**	**Width (m)**	**Surface Cover Type**	**Actual Constr. Year**	**Est. Constr. Year**	**P-value**
Maeda	98.3	11.6	Forest	2006	2005	7.17E-6
Kuroyama	98.0	8.3	Forest	1997	1996	2.00E-6
Nagasaka	96.0	11.0	Forest	2000	1999	8.31E-6
Higashi Ebara	82.0	11.0	Forest	2003	2000	3.14E-9
Osuji	64.0	12.0	Forest	1992	1989	1.30E-2
Mijimai	56.7	7.0	Forest	1994	1995	1.21E-6
Higashiri	51.0	11.2	Forest	1997	1995	4.90E-6
Daikan	43.0	13.3	Forest	1992	1989	5.89E-3
Nagamata	42.0	11.5	Forest	1998	1996	1.85E-11
Kamifukuchi	37.0	11.5	Forest	1992	1992	1.29E-6

Continued on next page

Table 6 – continued from previous page

Bridge Name	**Overall Length (m)**	**Width (m)**	**Surface Cover Type**	**Actual Constr. Year**	**Est. Constr. Year**	**P-value**
Makiya No.3	24.2	16.8	Forest	1991	1990	6.48E-6
Kamiyama	23.0	11.0	Forest	1993	1992	2.26E-4
Fukushi	21.8	5.0	Forest	1992	1991	4.02E-3
Second Geya	9.5	4.0	Forest	1996	1991	1.19E-2
Kamiyamatogawa	11.0	14.8	Forest	1992	—	—
Shitayamatogawa	11.0	14.8	Forest	1992	—	—
Blacksmith	33.9	6.5	Cropland	1992	1992	1.09E-3
Gabusoka	32.4	12.8	Cropland	1996	1993	1.35E-6
Haishi	27.9	12.5	Cropland	2002	1999	1.42E-6
Inada	30.6	5.5	Cropland	2003	1999	8.35E-7
Fukumi	70.0	11.0	Cropland	1992	2008	1.02E-4
Hane 105-2	31.0	6.0	Cropland	1993	1992	4.56E-3
Kayang Mata	22.3	5.0	Cropland	2001	2008	4.94E-3
Oura	77.0	15.8	Built-Up	1996	1997	9.63E-3
Higashi Yabu	56.6	17.1	Built-Up	2000	1997	6.76E-11
Furushima	47.0	16.0	Built-Up	1999	1997	2.00E-8
Nazaki	44.6	8.0	Built-Up	1994	1994	5.87E-6
Nakaoji	33.3	16.2	Built-Up	1993	1991	7.18E-4
Yonagawa	31.5	22.5	Built-Up	1992	1991	6.07E-5
Makiya No 2	28.3	18.8	Built-Up	1991	1990	1.43E-6
Kado River	25.0	22.5	Built-Up	1993	1992	2.27E-4
Tamemata	23.5	15.3	Built-Up	1990	1991	6.77E-5
Anwa Minamizaki	21.5	22.5	Built-Up	1991	1991	1.99E-3
Ose	44.0	5.0	Built-Up	1993	1992	3.40E-3
Name 162-1	18.2	4.0	Built-Up	1994	1996	3.56E-4
Sugita	25.0	15.6	Built-Up	1999	1987	5.77E-10
Hanejioo	24.6	7.5	Built-Up	1990	1996	7.15E-6
Maehira	23.1	6.6	Built-Up	1992	2000	6.29E-4
Yabu	46.5	14.3	Built-Up	1991	1990	6.55E-2
Anada	15.9	22.0	Built-Up	1992	1995	4.10E-3
Apanuku	11.8	4.0	Built-Up	1996	1995	5.32E-5
Lower River	16.0	7.0	Built-Up	1993	—	—
Makiya No. 1	11.8	20.1	Built-Up	1991	—	—
Minato	11.5	15.7	Built-Up	2000	—	—

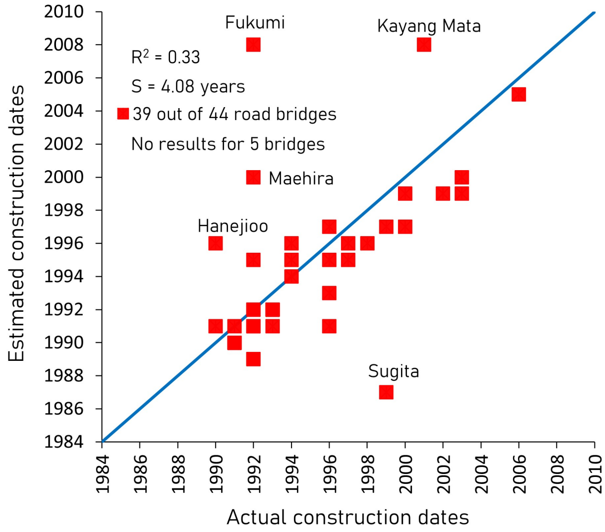

Figure 15: Estimated construction year versus actual construction year for the improved method at the TBP in Nago City

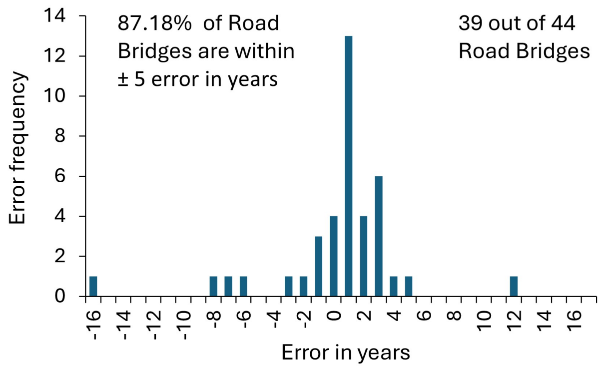

Figure 16: Error in Years for 39 out the 44 Road Bridges

2.10.3 Current and Previous Methods at Chaeng Meanchey Road Bridge

The previous and improved methods were compared, as shown in Figure 17. In Figure 17(a) and (b), the previous method was evaluated using the Normalized Difference Water Index (NDWI) and Normalized Difference Water Index 2 (NDWI_2),respectively, while in Figure 17(c) it was evaluated using the Normalized Difference Water Index 2 (NDWI_2). The results in Figure 17(a) and (b) are not clear, while the results are clear in Figure 17(c).

In Figure 17(c), the improved method using the NDWI_2 was analyzed and a Sequential

T-test Analysis of Regime Shift was used to identify regime shifts in the time series data. The results in Figure 17(c) are clear, and the method for determining the year of construction is objective.

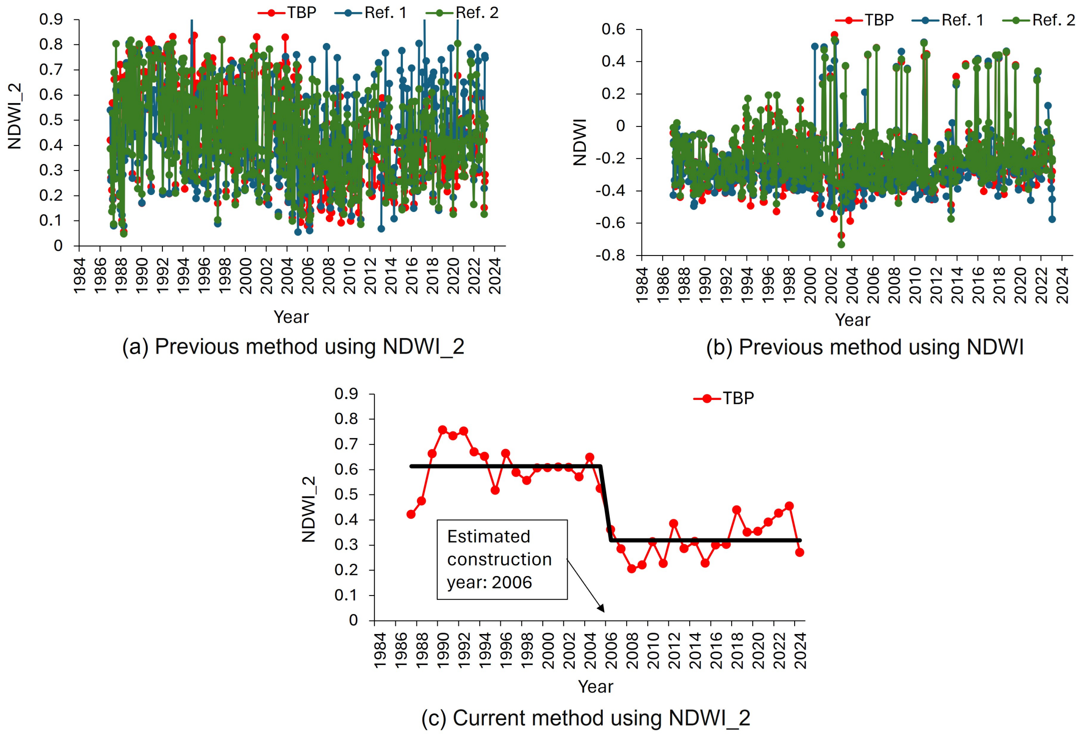

Figure 17: Results for the previous and improved methods

2.11 Conclusions

The improved method is an improvement on the previous method. The improved method successfully estimated the construction year of road bridges in Nago City by using the Normalized Difference Water Index 2 (NDWI_2) within Google Earth Engine and employing the Sequential T-test Analysis of Regime Shift to identify the optimal regime shift in the NDWI_2 time-series data. The identified optimal regime shift was then used as the estimated construction year of the road bridge.

Among the 12 indices evaluated, the Normalized Difference Vegetation Index, Normalized Difference Water Index 2, Blue Normalized Difference Vegetation Index, and Built-up Index recorded relatively high absolute mean differences, indicating their effectiveness in estimating the construction year.

The previous method was not clear and relied on subjective criteria for determining the estimated construction year. In contrast, the improved method is clear and employs an objective approach. However, it should be noted that seasonal variations and inadequate reflectance may lead to inaccurate or lack of results for some road bridges.

The results of this study show that the estimated year of construction is statistically significant when the p-value is below 0.05. Furthermore, the errors between the actual and estimated year of construction follow a normal distribution and most of the errors are close to zero. This indicates that the estimation method used is likely to be accurate and reliable. Future research could further investigate the factors affecting the accuracy of the estimation and further validate the performance of the model in different datasets or contexts.

Chapter 3

3 Application of the Improved Method on Road Bridges in Cambodia

3.1 Introduction

Effective bridge asset management and maintenance rely on a comprehensive database containing detailed information about each bridge, including its length, materials, construction date, and other relevant details. Cambodia recognized the importance of such a database and initiated a survey to collect this data for all road bridges. Between 2015 and 2017, Cambodian engineers conducted the first round of bridge inspections, revealing significant information gaps, notably the absence of construction years for 46% of the 2439 road bridges inspected [34].

Bridges are the backbone of a country's infrastructure, and accurate knowledge of their construction year is crucial for ensuring their safety and longevity The construction year provides valuable insights into a bridge's age, condition, and potential vulnerabilities, enabling bridge authorities to prioritize maintenance and repairs, allocate resources effectively, and make informed decisions about bridge replacement or upgrading.

This study proposes to assess the performance of an improved method for estimating the construction year of road bridges in Cambodia. The study utilized remote sensing data from Landsat 5 Thematic Mapper in Google Earth Engine (GEE) for data processing and analysis. The Sequential T-test Analysis of Regime Shift (STARS) method was utilized to identify the estimated construction year from the analyzed NDWI_2. The NDWI_2 is a function of near-infrared (NIR) and shortwave infrared 2 (SWIR2) bands, mathematically expressed as: NDWI_2 = (NIR - SWIR2)/(NIR + SWIR2). Data processing in GEE involves noise reduction and the mitigation of seasonal variations, to ensure the accuracy of the estimates. By leveraging the capabilities of GEE, the method can efficiently handle large datasets and provide consistent results.

The improved method will be applied to 649 road bridges in Cambodia, with an overall length less than or equal to 100 meters, and demonstrate the effectiveness of the method in estimating the construction year of road bridges. The results of a previous study on 100 road bridges in Cambodia will be compared with the results of the improved method in this study, highlighting the advantages and limitations of both approaches [34].

The improved method for estimating the construction year of road bridges in Cambodia will address the significant gaps in providing a comprehensive database with year of construction of road bridges. The accurate estimation of the construction year provides valuable insights for bridge maintenance and improvement, ensuring the safety and integrity of Cambodia's bridge infrastructure.

3.2 Road Bridges in Cambodia

Cambodia has about 2,439 road bridges according to the authority of the Road Infrastructure Department of the Ministry of Public Works and Transport. According to a survey conducted between 2015 and 2017, the construction year is unknown for 46% of these road bridges [34].

3.2.1 423 Road Bridges in Cambodia

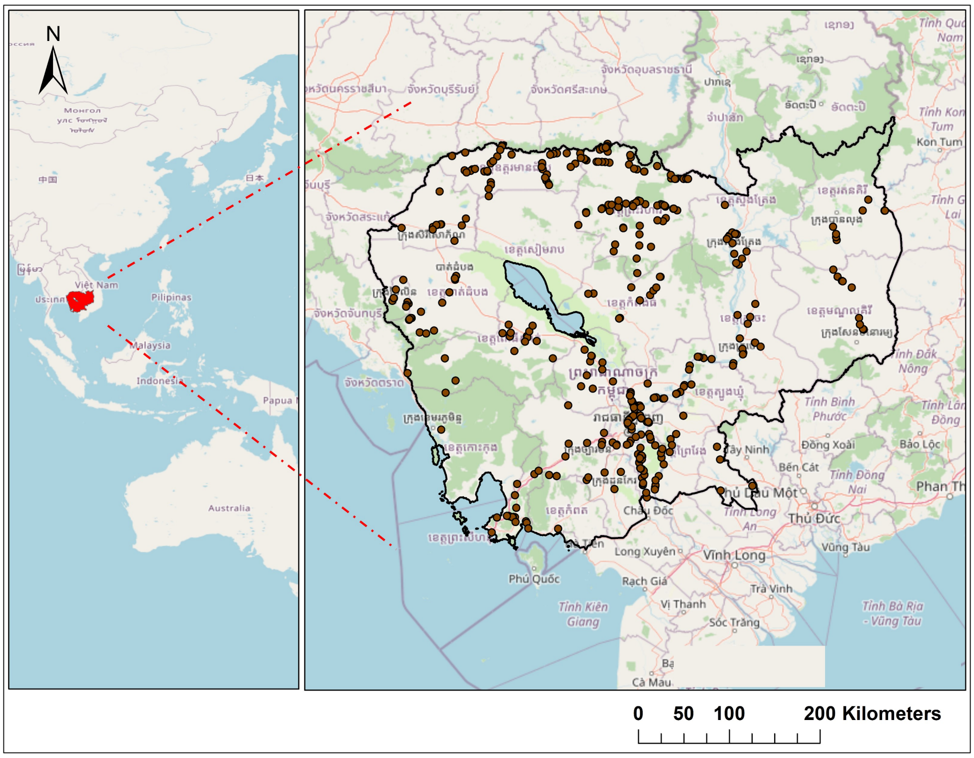

Figure 18: 423 Road Bridges in Cambodia of Overall Length ≤ 100 m

From the total of 2,439 road bridges, 649 road bridges with an overall length $\leq$ 100 m and known years of construction were examined in this study. Out of these 649 road bridges, 136 had missing results, 90 had no results, and 423 had complete results.

Figure 18 presents the 423 road bridges in Cambodia with an overall length $\leq$ 100 m that were analyzed in this study. The Normalized Difference Water Index 2 (NDWI2) was used to analyze these 423 road bridges in Google Earth Engine. After the analysis, the Sequential T-test Analysis of Regime Shift (STARS) was used to identify the estimated year of construction for each bridge.

3.2.2 100 Road Bridges in Cambodia of Overall Length between 20 m and 100 m

Table 7 presents 100 road bridges with overall lengths between 20 m and 100 m, together with their known years of construction. These 100 road bridges were initially analyzed using the previous method using the Normalized Difference Water Index (NDWI), a function of near-infrared (NIR) and visible green light, mathematically expressed as

$$\text{NDWI} = \frac{\text{NIR} - \text{Visible Green}}{\text{NIR} + \text{Visible Green}}.$$

The 100 road bridges in Table 7 will be re-analyzed using the improved method using the Normalized Difference Water Index 2 (NDWI_2), a function of near-infrared (NIR) and shortwave infrared 2 (SWIR2), mathematically expressed as

$$\text{NDWI\_2} = \frac{\text{NIR} - \text{SWIR2}}{\text{NIR} + \text{SWIR2}}.$$

Thereafter, the Sequential T-test Analysis of Regime Shift was used to determine the estimated year of construction. After the analysis, the results from the previous method and the improved method will be compared.

Table 7: 100 Road Bridges in Cambodia of Overall Length between 20 m and 100 m

Bridge Name	**Overall Length (m)**	**X - Coordinates**	**Y - Coordinates**	**Actual Construction Year**
Prek Kongvann	97.0	104.9820504595	11.7184709832	2011

Continued on next page

Table 7 – continued from previous page

Bridge Name	Overall Length (m)	X - Coordinates	Y - Coordinates	Actual Construction Year
Slaket	90.0	103.2126029396	13.1145862129	2009
Chaeng Meanchey	90.0	103.0752958413	12.8485632355	2006
Kbal Ro Meas	90.0	104.2237869320	10.6112208344	2007
Watpoo Sovanrangsay	90.0	103.9377884526	12.5647969950	2012
Prak Stay	85.0	103.9157733649	12.5184535187	2009
Thnol Dach	84.0	105.2671648817	11.9835194711	2010
Veng	84.0	104.5223319196	11.1195273767	2013
Hun Sen Terk Vel	84.0	105.7978171848	11.4235309437	2001
Chhay Luk	83.0	103.2074147232	12.0781968565	2013
Sra Aem	80.0	104.7330859762	14.2372419105	2012
Ta Eak	75.0	105.0327790109	11.8307224040	2007
Tekleach	75.0	104.0182188473	12.4736563685	2013
Prek ror luos	75.0	103.6184554854	10.7228774785	2002
Se Sen	75.0	102.9818491507	13.5742140769	2003
Prek Bat Dei	75.0	105.5445989024	12.0389599174	2009
Prek tmey	75.0	105.2599637337	11.1795909418	2011
Thmor Ta Khmao	72.0	104.9433012692	11.4842792670	2008
Borribau	72.0	104.4865119979	12.3845477737	2004
Aja tnorl	72.0	106.0008191276	12.7282926198	2013
Prak Kork	72.0	105.5292599493	12.2279158452	2003
O Tr Las 1	72.0	105.8761579442	13.8187036213	2012
O Romdoul	72.0	105.2073959325	13.6652895398	2014
Thmor Koul	72.0	105.4688350617	12.0181536530	2002
Prek somroung	70.0	105.0425834267	11.8138611852	2001
Cha Brong	63.0	104.4515355028	12.0209704177	2003
Prak Tayi	63.0	105.6666556306	12.3016543314	1993
Prek ta keo	61.0	105.2745406347	11.9012267310	2004
Knatangyoo	60.0	105.1032187153	10.9216314260	2015
Som Pong 1	60.0	105.1358634652	11.5199921642	2015
Som Pong 2	60.0	105.1338864325	11.5169320136	2015
Beoung Ray	60.0	105.7451590654	12.2912950531	2012
Kro Sang	60.0	105.7179385535	11.5351084577	2011
Ban Teay Staung	60.0	104.6427012047	12.9319113647	2006
Kbal chreus	60.0	103.7169565569	10.7378873406	2002
Anu Virak Salakrao	60.0	102.6172552952	12.9802560916	2009
Pang Rolim	60.0	102.7180172959	12.8092859296	2001

Continued on next page

Table 7 – continued from previous page

Bridge Name	**Overall Length (m)**	**X - Coordinates**	**Y - Coordinates**	**Actual Construction Year**
Kork Thom 1	57.0	102.6737878188	13.5923053811	2014
Doun Soy	56.5	106.0547385571	10.9608062103	2013
Prek Jek	56.0	106.0442378701	12.3143511916	2011
Term Pou	56.0	105.1769608214	11.9079965275	2004
Prek Rers	55.0	105.9559087734	12.2255940208	2000
Spean Bak	54.0	104.9047546111	11.4439627010	1990
Prek Chen	54.0	105.0308251841	11.2801228515	2009
Spean Sor	52.0	106.0247425814	12.4951894187	2010
O Trolok	52.0	105.0267731141	13.4136434121	2011
Kchorb	51.0	105.3657886609	11.6029809352	1998
Kvang	50.0	105.1450784914	13.4030990463	2008
Samroung	50.0	105.1411191809	11.4935169199	2002
O van thea	50.0	105.9107590770	13.5006711549	2011
Bom Nok	49.0	104.1719081162	12.2993802842	2007
Tang Houng	48.0	104.3288047903	11.4537916886	2006
Daun Sor	48.0	105.7239860422	11.2204739393	2006
Mer bon	48.0	105.3939685559	11.5491427417	2015
Prak Svay	45.0	105.4008090243	11.9486199427	2015
Jong tnorl	45.0	104.7818917132	11.0041208808	2012
Steung som bou krom	45.0	104.2090293408	11.1331788801	2009
Kom Raeng	45.0	105.7148882623	11.5364305998	2012
Brasat	45.0	105.1358960963	12.9243445875	2005
Jreav	45.0	106.2609479222	11.9548357692	2014
Banteay Youn	45.0	104.0072624200	12.6239465360	2008
Chheb	45.0	105.4032966025	13.7637083386	2010
O Torsur	45.0	105.2628657450	13.6572994574	2011
Bordersomroungpreyka	40.0	104.8454674283	11.1731725395	1997
Kon Dom Rey	39.0	102.6770285940	13.6192755826	2014
Thmat Pong	36.0	104.6788124153	11.5603439958	2004
Prak Svay	36.0	105.4733193848	12.0283079294	2002
Trey totoung	36.0	105.2643248599	11.8993343317	2004
Prek Ah Teang	36.0	105.1720233910	11.9056787242	2004
Bak Prea	36.0	105.7220619521	11.2982461103	2006
Thnout	36.0	105.7101886967	11.4867414022	2006
Phum Chik Dey	36.0	105.7255272227	11.5652638443	2013
Oh Prek	36.0	105.9851798076	13.5294154567	2013

Continued on next page

Table 7 – continued from previous page

Bridge Name	**Overall Length (m)**	**X - Coordinates**	**Y - Coordinates**	**Actual Construction Year**
Prek Thei Ka khpos	36.0	105.0047859260	11.3952407874	1990
Lvea Ta	35.0	105.0459762373	11.8355545431	2014
Prey chhrouv	30.0	104.3237390817	11.8330547560	2003
Prek Thmei	30.0	105.1899296978	11.0910377074	2009
Prek Tahing	30.0	105.2337507208	11.1600559740	2002
Watt Steung	30.0	104.5408876356	12.2685345156	2001
Prek Banhchhav	30.0	105.1862116040	11.0252085180	2010
Prek Tup	30.0	105.1896831867	11.0437483168	2010
Prek reus 1	30.0	105.0227849532	11.8299574097	2011
Preakthorng	30.0	104.9519917342	11.6249636437	2012
Spean 1	29.5	104.7092702490	14.3943127464	2011
Spean 2	29.5	104.7067418976	14.3924070561	2011
Spean 3	29.9	104.7024559109	14.3895915388	2014
Oh kop 2	28.0	107.2974886863	13.8703685752	2012
Krom leak	27.0	105.1039707507	11.6701232435	2003
Trorpen kro goug	25.5	104.4777666353	11.0832340695	2004
Chrok Sang Kae	25.0	104.5503417508	11.7814995217	2001
O Trokoun	24.0	104.5547827900	12.2196347520	2009
Kong srun	24.0	105.0792411179	11.1449241673	2012
Krang Tamom	24.0	104.5075660928	12.1300216717	2013
Au TangPil	24.0	104.4479899740	11.6208149033	2012
Phum Jey	24.0	104.9800722882	12.8413798118	2001
Vat Sethey	20.0	104.6712590801	11.8757155913	2002
O Thnol 1	20.0	105.0330669766	13.5742549188	2011
O Thnol 3	20.0	105.0320215284	13.6025655581	2012
Kok romLor	20.0	103.6723200775	12.5480328184	2012
Domnak Konseng	20.0	103.7454658532	12.5146654063	2014

3.3 Results and Discussion

3.3.1 Results of the 423 Road Bridges in Cambodia

The analysis of 423 road bridges in Cambodia was conducted using the improved method. The overall length of the 423 road bridges is $\leq$ 100 m. The improved method uses the

Normalized Difference Water Index 2 (NDWI_2). (NDWI_2) is a function of near-infrared (NIR) and shortwave infrared 2 (SWIR2), mathematically expressed as

$$\text{NDWI\_2} = \frac{\text{NIR} - \text{SWIR2}}{\text{NIR} + \text{SWIR2}}.$$

The regression analysis of the 423 road bridges is presented in Figure 19. The results are divided into three categories according to the range of the absolute mean error: low, medium, and high absolute mean error. The low category ranges from 0 to 5 absolute errors, the medium category from 6 to 10 absolute errors, and the high category from 11 to 30 absolute errors.

The results in Figure 19 recorded a high absolute mean error of 64.30% for the analyzed road bridges, suggesting that the construction years for 64.30% of the 423 road bridges in Cambodia were accurate and reliable.

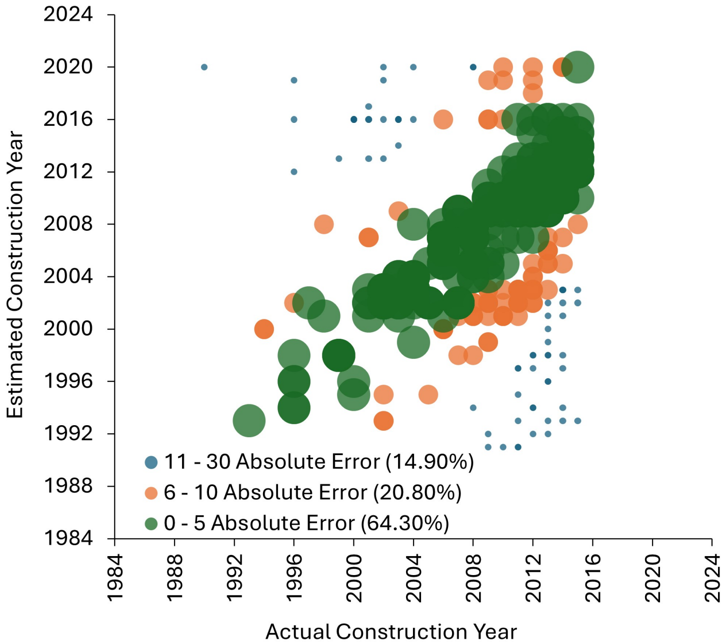

Figure 19: Estimated Construction Year versus Actual Construction Year for the Improved Method at 423 Road Bridges in Cambodia

The recorded R^2 for the 423 road bridges is 0.06. The low R^2 values could be attributed to insufficient reflectance due to atmospheric absorption and scattering effects. In addition, differences between the planned year of construction recorded in the database and the actual year of construction may have contributed to the discrepancy between the estimated and actual years, resulting in lower R^2 values. Such discrepancies may have been caused by construction delays.

The recorded absolute mean error for all the 423 road bridges is 4.93 years, suggesting that the results are accurate and the method is reliable. The distribution of the errors is presented in Figure 20. According to the results in Figure 20, the histogram follows a normal distribution, with most errors being close to zero. This indicates that the predictions of the model are likely to be accurate and reliable.

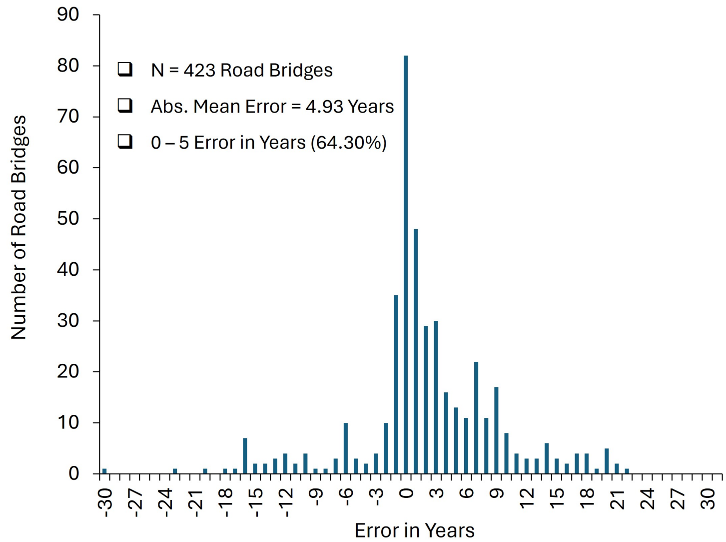

Figure 20: Error in Years for 423 Road Bridges in Cambodia

It was observed that with the increase in the overall length of the road bridge, the absolute mean values decrease, as shown in Figure 21.

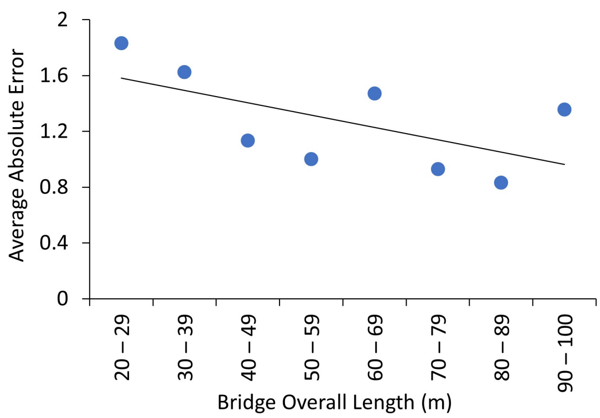

Figure 21: 423 Road Bridges in Cambodia of Overall Length less or equal to 100 Meters

This could be due to an increase in the surface area of the road, which enhances visibility and thus increases the accuracy of the results.

It was observed that the estimated construction years for road bridges with high errors (11 to 30 years) were either at the start or the end of the time series data, as shown in Figures 19 and 20. To further understand the distribution of the errors on the surface area of Cambodia, a plot of all errors from 0 to 30 were conducted as shown in Figure 22(a), low error (0 to 5 years) in Figure 22(b), medium error (6 to 10 years) in Figure 22(c), and high error (11 to 30 years) in Figure 22(d). There was still no discernible trend even for the high-error bridges on the map, as shown in Figure 22(d). Therefore, further research is needed to understand the cause of this behavior and to develop techniques to reduce these errors.

It was observed that the estimated construction years for road bridges with high errors (11 to 30 years) were either at the start or the end of the time series data, as shown in Figures 19 and 20.

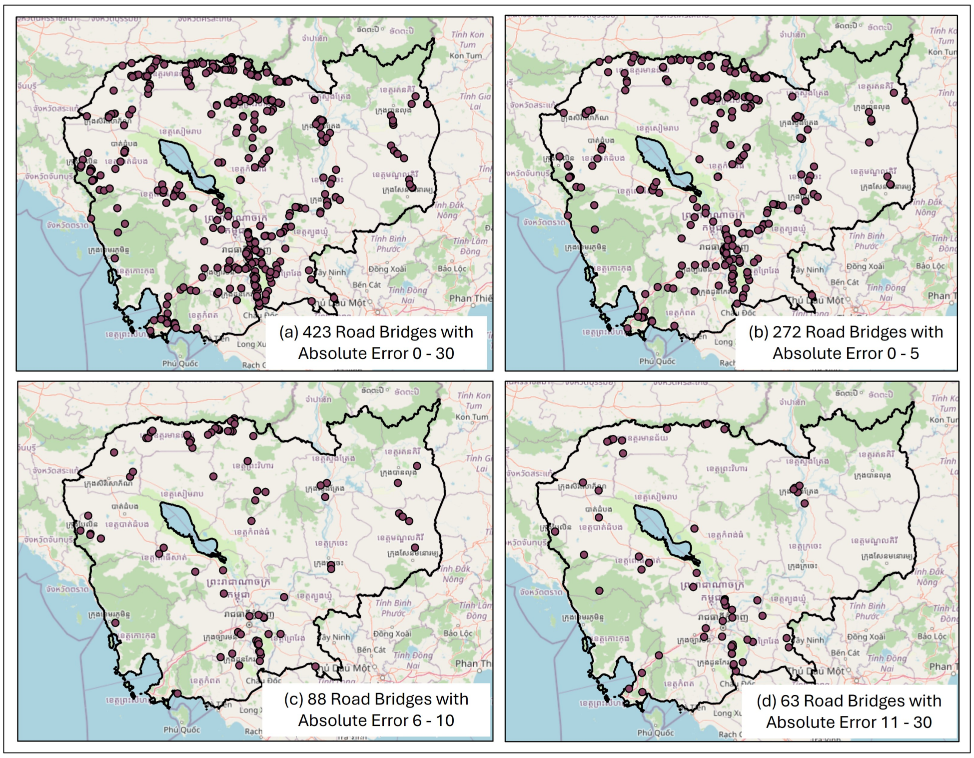

Figure 22: 423 Road Bridges in Cambodia of Overall Length less or equal to 100 Meters

To further understand the distribution of the errors across the surface area of Cambodia, a plot of all errors from 0 to 30 years was conducted, as shown in Figure 22(a). Additionally, plots for low errors (0 to 5 years) are shown in Figure ??(b), medium errors (6 to 10 years) in Figure 22(c), and high errors (11 to 30 years) in Figure 22(d). There was still no discernible trend even for the high-error bridges on the map, as shown in Figure 22(d). The overall length of the road bridges with high absolute error (11 to 30 years) is between 20 m and 100 m. Therefore, further research is needed to understand the cause of this behavior and to develop techniques to reduce these errors.

3.3.2 Comparison of the Previous Method and the Improved Method on the 100 Road Bridges in Cambodia

The results of the previous method and the improved method are shown in Table 8. Under the columns for the improved method results and comments in Table 8, 12 road bridges recorded no results, and 11 road bridges had a p-value greater than 0.05. This suggests that the no results record could have been due to inadequate reflectance, and the p-value greater than 0.05 indicates that the shifts are insignificant.

To enable a fair comparison between the two methods, the previous method was also reduced by 12 road bridges corresponding to the no results records for the improved method. Therefore, 88 road bridges were compared between the previous method and the improved method.

Table 8: Results of the Previous Method and Improved Method on the 100 Road Bridges in Cambodia of Overall Length between 20 m and 100 m

Bridge Name	Overall Length (m)	Actual Constr. Year	Est. Constr. Year (Previous Method)	Est. Constr. Year (Improved Method)	Comments - Improved Method
Prek Kongvann	97.0	2011	2014	—	no result
Slaket	90.0	2009	2011	2009	
Chaeng Meanchey	90.0	2006	1988	2006	
Kbal Ro Meas	90.0	2007	1988	2006	
Watpoo Sovanrangsay	90.0	2012	1988	2013	
Prak Stay	85.0	2009	1988	2009	
Thnol Dach	84.0	2010	2010	—	no result
Veng	84.0	2013	2013	2007	
Hun Sen Terk Vel	84.0	2001	1988	2016	

Continued on next page

Table 8 – continued from previous page

Bridge Name	**Overall Length (m)**	**Actual Constr. Year**	**Est. Constr. Year (Previous Method)**	**Est. Constr. Year (Improved Method)**	**Comments - Improved Method**
Chhay Luk	83.0	2013	2011	1996	
Sra Aem	80.0	2012	1988	2010	p-value > 0.05
Ta Eak	75.0	2007	1988	2007	
Tekleach	75.0	2013	1988	2001	
Prek ror luos	75.0	2002	1988	2019	
Se Sen	75.0	2003	1992	2001	
Prek Bat Dei	75.0	2009	1988	2009	
Prek tmey	75.0	2011	2010	2012	
Thmor Ta Khmao	72.0	2008	2006	2008	
Borribau	72.0	2004	1988	2002	
Aja tnorl	72.0	2013	2007	2013	
Prak Kork	72.0	2003	2003	2004	p-value > 0.05
O Tr Las 1	72.0	2012	1988	2011	
O Romdoul	72.0	2014	2009	2015	
Thmor Koul	72.0	2002	2003	2002	
Prek somroung	70.0	2001	1988	2016	
Cha Brong	63.0	2003	2001	2002	
Prak Tayi	63.0	1993	1988	1993	
Prek ta keo	61.0	2004	1988	1999	
Knatangyoo	60.0	2015	1988	2015	
Som Pong 1	60.0	2015	1988	2016	
Som Pong 2	60.0	2015	1988	2014	
Beoung Ray	60.0	2012	2009	2013	
Kro Sang	60.0	2011	2005	2010	
Ban Teay Staung	60.0	2006	1988	—	no result
Kbal chreus	60.0	2002	1993	2003	
Anu Virak Salakrao	60.0	2009	2010	2009	
Pang Rolim	60.0	2001	1988	2007	
Kork Thom 1	57.0	2014	1988	1997	
Doun Soy	56.5	2013	1997	2012	
Prek Jek	56.0	2011	1988	2003	
Term Pou	56.0	2004	2003	2004	
Prek Rers	55.0	2000	1997	1996	
Spean Bak	54.0	1990	1988	2020	

Continued on next page

Table 8 – continued from previous page

Bridge Name	**Overall Length (m)**	**Actual Constr. Year**	**Est. Constr. Year (Previous Method)**	**Est. Constr. Year (Improved Method)**	**Comments - Improved Method**
Prek Chen	54.0	2009	2003	—	no result
Spean Sor	52.0	2010	2005	2009	
O Trolok	52.0	2011	1988	2010	p-value > 0.05
Kchorb	51.0	1998	1993	—	no result
Kvang	50.0	2008	1988	2001	
Samroung	50.0	2002	2001	2002	
O van thea	50.0	2011	2014	1995	
Bom Nok	49.0	2007	1988	2001	
Tang Houng	48.0	2006	2004	2006	
Daun Sor	48.0	2006	1988	2004	p-value > 0.05
Mer bon	48.0	2015	1988	2014	
Prak Svay	45.0	2015	1988	2008	
Jong tnorl	45.0	2012	2008	2002	
Steung som bou krom	45.0	2009	2008	2004	
Kom Raeng	45.0	2012	2006	2015	
Brasat	45.0	2005	1988	2005	
Jreav	45.0	2014	2006	1996	
Banteay Youn	45.0	2008	1988	2019	
Chheb	45.0	2010	1988	2010	
O Torsur	45.0	2011	1988	2010	
Bordersomroungpreyka	40.0	1997	1988	2002	p-value > 0.05
Kon Dom Rey	39.0	2014	2011	1990	p-value > 0.05
Thmat Pong	36.0	2004	1988	2020	
Prak Svay	36.0	2002	2003	2002	
Trey totoung	36.0	2004	2003	2004	
Prek Ah Teang	36.0	2004	2003	2003	
Bak Prea	36.0	2006	1996	—	no result
Thnout	36.0	2006	1997	2006	
Phum Chik Dey	36.0	2013	1996	2013	
Oh Prek	36.0	2013	1988	2010	
Prek Thei Ka khpos	36.0	1990	1994	1990	p-value > 0.05
Lvea Ta	35.0	2014	1988	—	no result
Prey chhrouv	30.0	2003	2004	2004	
Prek Thmei	30.0	2009	1988	1992	

Continued on next page

Table 8 – continued from previous page

Bridge Name	**Overall Length (m)**	**Actual Constr. Year**	**Est. Constr. Year (Previous Method)**	**Est. Constr. Year (Improved Method)**	**Comments - Improved Method**
Prek Tahing	30.0	2002	1988	—	no result
Watt Steung	30.0	2001	1988	2002	
Prek Banhchhav	30.0	2010	2003	—	no result
Prek Tup	30.0	2010	1988	2010	
Prek reus 1	30.0	2011	2013	2011	
Preakthorng	30.0	2012	1988	2009	
Spean 1	29.5	2011	1988	2011	
Spean 2	29.5	2011	1988	2010	
Spean 3	29.9	2014	2005	2003	
Oh kop 2	28.0	2012	2003	1991	p-value > 0.05
Krom leak	27.0	2003	1988	2003	
Trorpen kro goug	25.5	2004	2000	2004	
Chrok Sang Kae	25.0	2001	1988	—	no result
O Trokoun	24.0	2009	1988	2002	p-value > 0.05
Kong srun	24.0	2012	2010	2018	
Krang Tamom	24.0	2013	1988	2017	
Au TangPil	24.0	2012	1988	1991	p-value > 0.05
Phum Jey	24.0	2001	1988	—	no result
Vat Sethey	20.0	2002	2003	—	no result
O Thnol 1	20.0	2011	1988	2010	
O Thnol 3	20.0	2012	1988	2010	p-value > 0.05
Kok romLor	20.0	2012	1988	2001	
Domnak Konseng	20.0	2014	2003	2015	

The regression analysis of the previous method and the improved method on the 88 road bridges are presented in Figures 23. The recorded R^2 values for both methods are low, with the R^2 value for the improved method being higher than that of the previous method. The low R^2 values could be attributed to insufficient reflectance due to atmospheric absorption and scattering effects. Additionally, discrepancies between the planned year of construction recorded in the database and the actual year of construction may have contributed to the differences between the estimated and actual years, resulting in lower R^2 values. Such discrepancies may have been caused by construction delays.

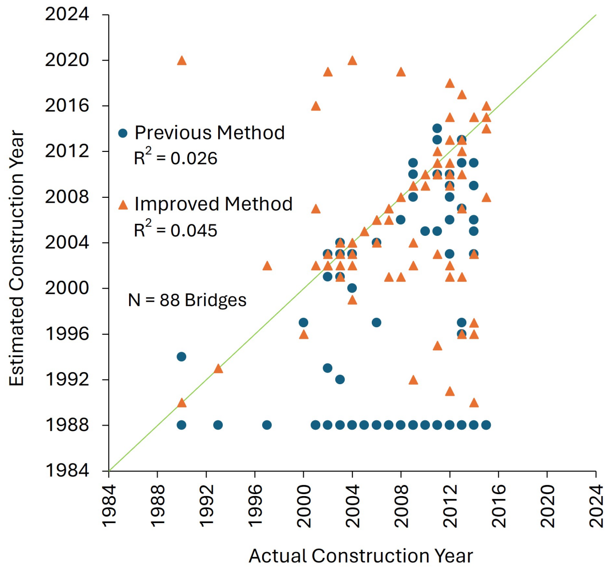

Figure 23: Estimated Construction Year versus Actual Construction Year for both Methods at 88 Road Bridges in Cambodia

As was the case for the estimated construction years at the start and end of the NDWI_2 time series data, the 88 road bridges for both methods also experienced similar estimated construction years at the start and end of the NDWI_2 time series data. For absolute mean errors between 11 and 30 years, the previous method recorded 55.68% of the 88 road bridges, as shown in Figure 24(a), while the improved method recorded 19.32%, as shown in Figure 24(b). The cause of this behavior will be investigated in future research.

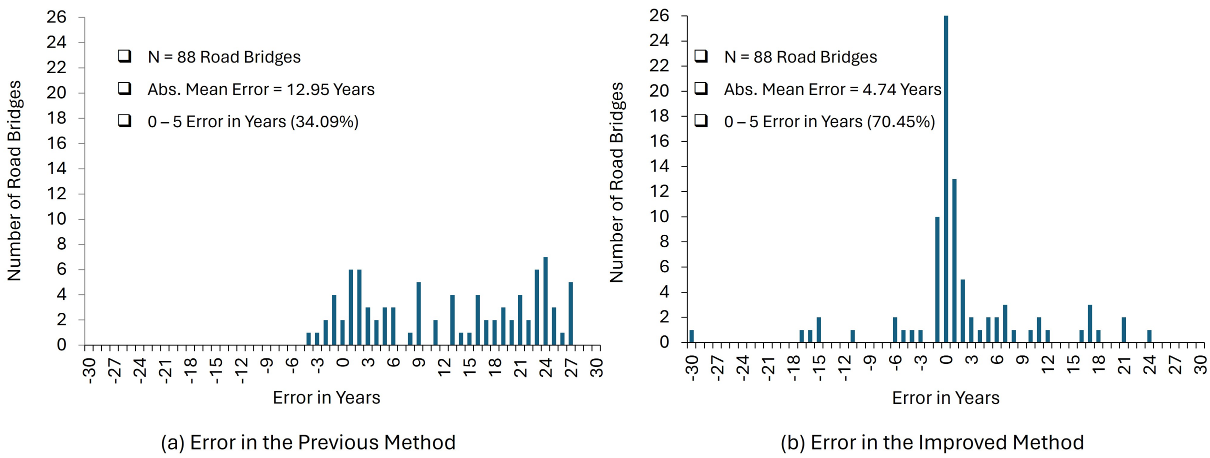

Figure 24: Error in Years for the Previous Method and Improved Method at 88 Road Bridges in Cambodia

An absolute mean error for all the 88 road bridges recorded was 12.95 years for the previous method and 4.74 years for the improved method. According to the results in Figure 24(b), the histogram for the improved method follows a normal distribution, with most errors being close to zero, while the histogram for the previous method in Figure 24(a) is shifted to the right and exhibits a bimodal distribution, indicating that the data may have two populations. The absolute error from 0 to 5 years for the improved method accounts for 70.45%, higher than the 34.09% in the previous method, as shown in Figures 24(b) and 24(a), respectively. Based on the relatively small absolute error and the normal distribution behavior, this suggests that the predictions of the improved method are likely to be more accurate and reliable than the previous method. The bimodal behavior of the previous method requires further research to understand the cause.

3.4 Conclusions

The improved method is an improvement of the previous method. The improved method successfully estimated the construction year of the road in Cambodia by using the Normalized Difference Water Index 2 (NDWI_2) within Google Earth Engine and employing the Sequential T-test Analysis of Regime Shift to identify the optimal regime shift in the NDWI_2 time-series data. The identified optimal regime shift was then used as the estimated construction year of the road bridge.

There is a relationship between the overall length of the road bridge, and the absolute mean errors. An increase in the overall length of the road bridge, decreases the absolute mean error in the estimated year of construction.

The improved method recorded a relatively low absolute mean error, and high R^2 than the previous method. The distribution of the error for the improved method is normally distributed, an indicator that the model is likely accurate and reliable.

High absolute mean errors were observed at the ends and the starts of the NDWI_2 time series data and this requires further research to understand its cause and how to remedy it. Bimodal distribution of error shifted to the right was observed in the estimated construction years of the previous, which also requires further research.

Chapter 4

4 Application of the Improved Method on Road Bridges in Zambia

4.1 Introduction

Bridges are the backbone of a country's infrastructure, and accurate knowledge of their construction year is crucial for ensuring their safety and longevity The construction year provides valuable insights into a bridge's age, condition, and potential vulnerabilities, enabling bridge authorities to prioritize maintenance and repairs, allocate resources effectively, and make informed decisions about bridge replacement or upgrading.

This study proposes to assess the performance of an improved method for estimating the construction year of road bridges in Zambia. The study utilized remote sensing data from Landsat 5 Thematic Mapper and Landsat 7 Enhanced Thematic Mapper Plus in Google Earth Engine (GEE) for data processing and analysis. The Sequential T-test Analysis of Regime Shift (STARS) method was utilized to identify the estimated construction year from the analyzed NDWI_2. The NDWI_2 is a function of near-infrared (NIR) and shortwave infrared 2 (SWIR2) bands, mathematically expressed as

$$\text{NDWI} = \frac{\text{NIR} - \text{Visible Green}}{\text{NIR} + \text{Visible Green}}$$

.

Data processing in GEE involves noise reduction and the mitigation of seasonal variations, to ensure the accuracy of the estimates. By leveraging the capabilities of GEE, the method can efficiently handle large datasets and provide consistent results.

The improved method will be applied to 27 road bridges in Zambia, 15 of which the year of construction is known and for the remaining 12, the year of construction is not known.

4.2 Road Bridges in Zambia

The study area is Zambia, located in the southern part of Africa, and is surrounded by eight countries, as shown in Figure 25. The total gazetted road network in Zambia is

67,671 km, of which 40,454 km comprises the core road network (CRN), and only 25% of the CRN is paved [66].

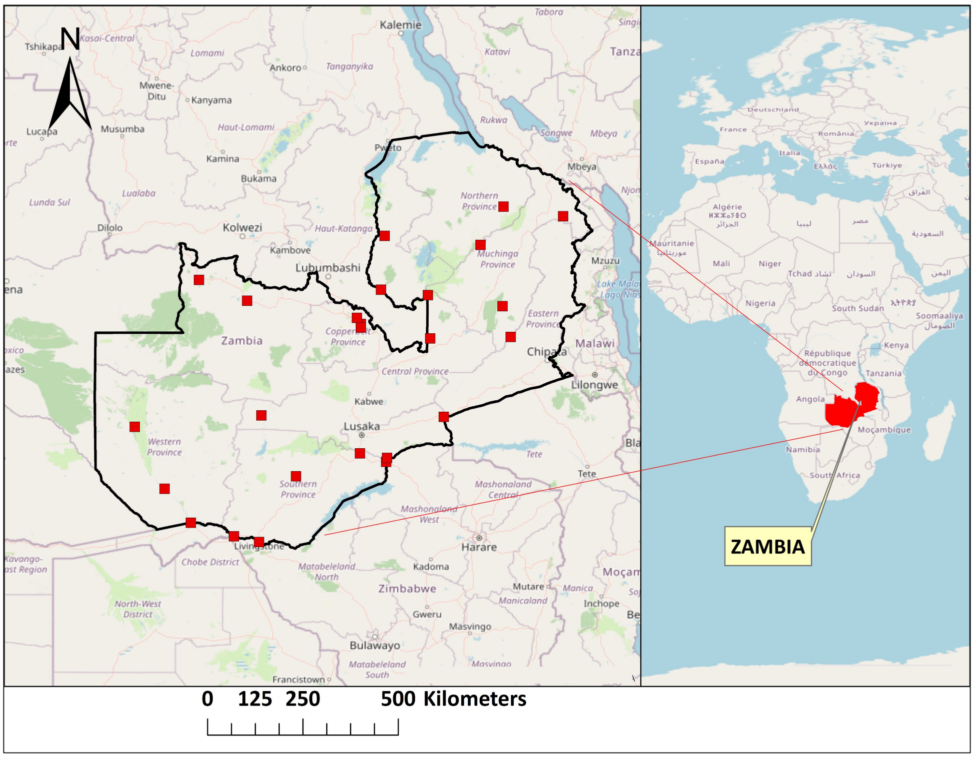

Figure 25: 27 Road Bridges on the core road network in Zambia

The CRN consists of trunk, main and district (TMD), urban, and primary feeder roads. The CRN is the barest road network which, if improved, will boost economic and social development and contribute to poverty reduction in Zambia [66]. There are over 460 major road bridges in Zambia (excluding culvert bridges) [67]. For over 90% of the road bridges in Zambia, the year of construction is not known, and, bridge's overall length is less than 100 meters. The 27 road bridges examined in this study and their distribution by road types are shown in Figure 25 and Table 9. The 27 road bridges were selected based on the availability of data and the importance of the road. Of the 27 road bridges, 15 road bridges have a known year of construction, while 12 have an unknown year of construction, as shown in Table 9.

Table 9: The characteristics of the 27 Road Bridges in Zambia

Bridge Name	Road Type	X-Coord.	Y-Coord.	Overall Length (m)	Actual Constr. Year
Makuku	District	29.834583	-12.112484	2700	—
Lubosi Imwiko	Unknown	22.926593	-15.214748	1022	2016 [68, 69]
Kazungula	Unknown	25.262468	-17.791052	923	2020 [66]
Katima Mulilo	Main	24.249183	-17.472127	877	2004 [70]
Chirundu	Trunk	28.851696	-16.038713	400	2002 [71]
Otto Beit	Trunk	28.852240	-16.037952	369	1939 [71]
Chembe	Main	28.730508	-11.984665	322	—
Luangwa	Trunk	30.212141	-14.975860	304	1968 [72, 73]
Kafue Hook	Main	25.913296	-14.944958	282	—
Sioma	Unknown	23.627272	-16.671806	252	2016 [68]
Chiawa	Feeder	28.875237	-15.945233	240	2014 [74]
Victoria Falls	Trunk	25.857264	-17.928281	198	1905 [75]
Kafue	Trunk	28.236934	-15.837427	162	1949 [76]
Mufuchani	Unknown	28.256883	-12.790290	160	2016 [68]
Unknown 1	District	31.786030	-13.097708	187	—
Unknown 2	Main	31.076868	-10.926352	175	—
Unknown 3	Main	28.813611	-10.715243	131	—
Unknown 4	District	33.022331	-10.251896	124	—
Unknown 5	Main	28.164414	-12.644588	107	—
Unknown 6	Trunk	28.257794	-12.877707	107	—
Unknown 7	Trunk	28.257808	-12.877958	106	—
Unknown 8	Trunk	24.438223	-11.753351	105	—
Unknown 9	Trunk	25.573890	-12.243236	105	—
Unknown 10	Feeder	31.595438	-12.374057	38	2008 [*]
Unknown 11	Feeder	26.724435	-16.381289	26	2009 [*]
Unknown 12	Feeder	31.617739	-10.028214	26	2009 [*]
Unknown 13	Feeder	29.892065	-13.132957	22	2010 [*]

Note: [*] The actual years of construction for the four road bridges were provided by the Road Development Agency in Zambia

4.3 Results and Discussion

The Normalized Difference Water Index 2 (NDWI_2), as shown in Equation (6), was used for the analysis of 27 road bridges in Zambia, which are listed in Table 9. The estimated years of construction and p-values for these Bridges are shown in Table 10. The results of the regression analysis are shown in Figure 26, and the distribution of the errors in Figure 27.

Figure 26 shows a moderate R^2 value of 0.64 and Figure 27 shows the distribution of the errors. An overall absolute mean error of 13.79 years for the 14 road bridges was recorded as shown in Table 10 and Figure 27. A moderate R^2 value of 0.64 was recorded, slightly higher than the 0.33 recorded in Nago City, and 0.06 recorded in Cambodia. The small sample size could have been one of the contributing factors to a relatively higher R^2 value of 0.64. The small sample was adopted because of lack of sufficient road bridges with known years of construction. An overall absolute mean error of 13.79 years was recorded, which was relatively higher than the 2.69 years recorded in Nago City and 4.93 years recorded in Cambodia. The three outliers (the results Victoria Falls, Otto Beit, and Luangwa road bridges) contributed to the error of 13.79 years, as shown in Figure 26, and Figure 27. About 80% of the 14 road bridges recorded an absolute error in the range 0 to 5 years, indicating that the results were accurate as shown in Figure 27.

In Table 9 the years of construction are known for 15 road bridges. Of these 15 road bridges, 12 road bridges recorded p-values of less than 0.05, indicating that the results were statistically significant. Figure 26 and Figure 27 identifies three outliers namely: Victoria Falls, Luangwa and Otto Beit. The Luangwa and Victoria Falls road bridges both recorded p-values greater than 0.05, suggesting that the regime mean shifts were statistically insignificant, possibly due to seasonal variation and insufficient reflectance. In contrast, the Otto-Beit road bridge recorded a p-value of less than 0.05 and a large absolute error of 60 years. The absolute error of 60 years is calculated from the difference between the estimated construction year of 1999 and the actual year of 1939, as shown in Table 10. This discrepancy could be due to interference from the neighboring Chirundu road bridge, whose estimated year of construction is 1999, as shown in Table 10. This phenomenon requires further research.

In Table 9 the years of construction for 12 road bridges were unknown. The years of construction were estimated for six of these road bridges, five of which recorded p-values of less than 0.05. The accuracy of the results for these five road bridges requires additional techniques to ensure the reliability of the results. No results were obtained for the remaining seven road bridges, as shown in Table 10, possibly due to seasonal variation and insufficient reflectance. Of the seven road bridges, four road bridges (Unknown 5, 6, 7, and 9) shown in Table 10, recorded an upward shift in Normalized Difference Water Index 2, which requires further investigation.

Table 10: Estimated construction years and p-values of the 27 Road Bridges in Zambia

Bridge Name	**Road Type**	**Overall Length (m)**	**Actual Constr. Year**	**Est. Constr. Year**	**P-value**
Makuku	District	2700	—	1993	2.23E-06
Lubosi Imwiko	Unknown	1022	2016	2013	2.15E-12
Kazungula	Unknown	923	2020	2017	3.71E-06
Katima Mulilo	Main	877	2004	2003	1.13E-13
Chirundu	Trunk	400	2002	1999	6.10E-12
Otto Beit	Trunk	369	1939	1999	1.43E-05
Chembe	Main	322	—	2008	9.17E-15
Luangwa	Trunk	304	1968	1993	9.00E-02
Kafue Hook	Main	282	—	1999	1.57E-06
Sioma	Unknown	252	2016	2015	4.46E-08
Chiawa	Feeder	240	2014	2013	8.63E-11
Victoria Falls	Trunk	198	1905	1994	2.01E-01
Kafue	Trunk	162	1949	—	—
Mufuchani	Unknown	160	2016	2014	1.55E-11
Unknown 1	District	187	—	2015	4.19E-02
Unknown 2	Main	175	—	2020	8.70E-01
Unknown 3	Main	131	—	—	—
Unknown 4	District	124	—	2001	1.69E-04
Unknown 5	Main	107	—	—	—
Unknown 6	Trunk	107	—	—	—
Unknown 7	Trunk	106	—	—	—
Unknown 8	Trunk	105	—	—	—
Unknown 9	Trunk	105	—	—	—
Unknown 10	Feeder	38	2008	2008	2.10E-09
Unknown 11	Feeder	26	2009	2009	1.06E-06
Unknown 12	Feeder	26	2009	2008	5.97E-05
Unknown 13	Feeder	22	2010	2014	1.57E-03

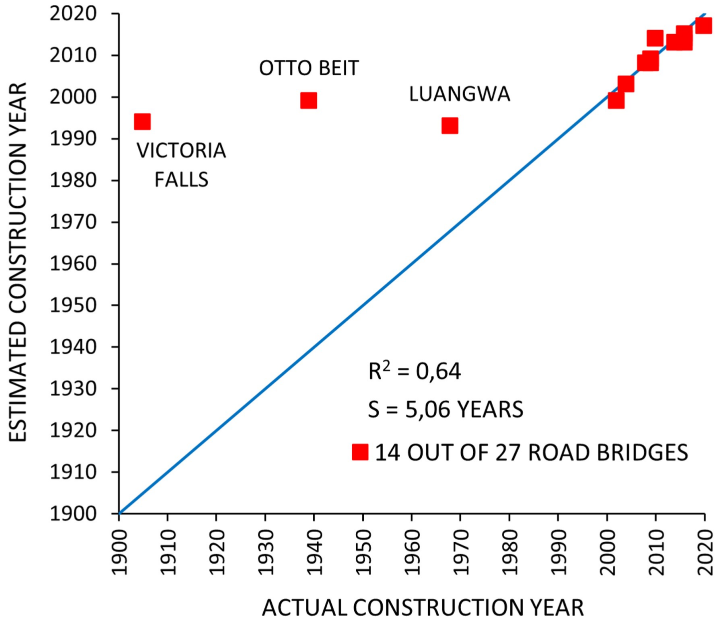

Figure 26: Estimated construction year versus actual construction year for the improved method at the TBP in Zambia

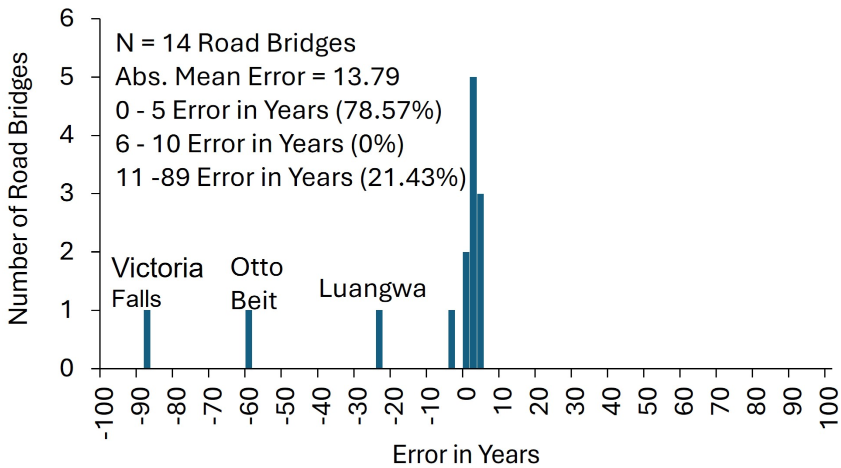

Figure 27: Error in Years for the Improved Method on 14 Road Bridges in Zambia

4.4 Conclusions

The Normalized Difference Water Index 2 (NDWI_2) in Google Earth Engine and the Sequential T-test Analysis of Regime Shift was used to estimate the year of construction of road bridges in Zambia. The relationship between the actual and estimated years of construction of The road bridges in Zambia was moderate and the results of the estimated year of construction were accurate. An upward shift of the NDWI_2 was observed in the results of the road bridges. The proximity of road bridges with different years of construction can lead to interference in the reflectance values, which affects the accuracy of the estimated year of construction. The relibility of the results for the road bridges with unkown year of construction was uncertain.

Chapter 5

5 Conclusions, Recommendations, and Significance of the Study

The improved method was successfully developed as an enhancement of the previous method. The improved method uses the Normalized Difference Water Index 2 (NDWI_2) in Google Earth Engine (GEE) to process and analyze the data. NDWI_2 is a function of near-infrared and shortwave infrared 2 bands. Landsat 5 Thematic Mapper and Landsat 7 Enhanced Thematic Mapper Plus are used to collect the near-infrared and shortwave infrared 2 bands within GEE. Data processing in GEE reduces noise and seasonal variations.

Among the 12 indices evaluated, the Normalized Difference Vegetation Index, Normalized Difference Water Index 2, Blue Normalized Difference Vegetation Index, and Built-up Index demonstrated relatively high absolute mean differences, indicating their effectiveness in estimating the construction year.

The estimated year of construction was successfully determined in Nago City, Japan, Cambodia, and Zambia, with low absolute mean errors and normally distributed errors in Japan and Cambodia, suggesting that the model is likely accurate and reliable. The R^2 values were low for all cases, which could have been caused by inadequate reflectance. Additionally, differences between the planned year of construction recorded in the database and the actual year of construction may have contributed to the discrepancy between the estimated and actual years, resulting in lower R^2 values. Such discrepancies may have been caused by construction delays. The limited number of bridges tested in Zambia was due to the insufficient availability of data on known years of construction.

A relationship was observed between the overall length of the road bridge and the absolute mean errors. An increase in the overall length of the road bridge decreases the absolute mean error in the estimated year of construction in the 0 to 5 years absolute error.

The improved method recorded lower absolute mean errors than the previous method, and the R^2 for the improved method was relatively higher than that of the previous method, suggesting that the improved method is more accurate.

The proximity of road bridges with different years of construction requires further research to investigate whether it can lead to interference in the reflectance values, thereby affecting the accuracy of the estimated year of construction.

High errors in the range of 11 to 30 years were observed for the estimated years of construction at the beginning and end of the NDWI_2 time series data for the road bridges in Cambodia. This phenomenon requires further investigation.

It was observed that the regime shift for the NDWI_2 was upward for some road bridges. This phenomenon requires further investigation.

To improve the practical utility of the model, future research efforts are needed to refine the methods, expand the data set, and develop techniques to increase the reliability of the downward shift results for road bridges with unknown years of construction. This includes the inclusion of comprehensive data on bridge renovations and new construction, each with verified years of construction.

For many road bridges with unknown construction years, the fully developed method will offer significant time and cost savings in estimating the construction years. This method serves as a valuable planning tool when the bridge age is combined with damage ratings to assess bridge deterioration rates. The resultant information can be used to:

- Forecast the future deterioration rates of road bridges;
- Schedule inspections of road bridges;
- Develop maintenance budgets for the road bridges; and
- Prioritize maintenance and repair works for critical road bridges that need immediate attention.

Additionally, its applicability extends beyond bridges, enabling the determination of construction years for various human-made structures.

References

[1] Yari, N. New model for Bridge Management System (BMS). Ph.D. Thesis, University of New Hampshire, Durham, NH, USA, 2018.

[2] Pregnolato M. Bridge safety is not for granted–A novel approach to bridge management *Engineering Structures* **2019** *196:109193*

[3] Joshi S, Thorat A, Dehadray H, Tundalwar M. Sustainability of Bridges: Risk Mitigation for Natural Hazards *Journal of Architectural Environment and Structural Engineering Research* **2023** *6(3):4-16*

[4] Jeon CH, Nguyen DC, Roh G, Shim CS. Development of brim-based bridge maintenance system for existing bridges *Buildings* **2023** *13(9):2332*

[5] Sastrawiria RP, Seigo N. The Intention of Bridge Asset Management Implementation in Indonesia. *Buildings* **2024** *14(3):622*

[6] Watanabe M, Ibayashi K, Goso T, Minagawa M. Challenges of bridge maintenance management in developing countries and nationwide practice of bridge database preparation system in Cambodia.*Journal of Japan Society of Civil Engineers* **2021** *77(1):70-83*

[7] Ahlskog JJ. Bridge management—The answer to the challenge. InBridge evaluation, repair and rehabilitation *Dordrecht: Springer Netherlands* **1990** 3-10

[8] Bień J, Salamak M. The management of bridge structures–challenges and possibilities. *Archives of Civil Engineering* **2022** 5-35.

[9] Hearn GE, Purvis RL, Thompson P, Bushman WH, McGhee KK, McKeel WT. Bridge Maintenance and Management: A look to the future. *InTRB 81st Annual Meeting: A3C06: Structures Maintenance and Management* **2000** 1-7

[10] Orcesi AD, Frangopol DM. Optimization of bridge management under budget constraints: Role of structural health monitoring. *Transportation research record* **2010** *2202(1):148-58*

[11] Orcesi A, Godart B, Gaillet L, Schmidt F, Bardou N, Limongelli MP, Carreaud P, Lenoir F, Baron FG. Technological developments as an answer to bridge management challenges.*InIABSE Symposium 2019, Towards a Resilient Built Environment-Risk and Asset Management* **2019** *8-p*

[12] Habeenzu H, McGetrick PJ, Hester D, Taylor SE. Bridge management systems-a review of the state of the art and recommendations for future practice. *Bridge Maintenance, Safety, Management, Life-Cycle Sustainability and Innovations* **2021** 926-33.

[13] Oppert ML, O'Keeffe V. The future of the ageing workforce in engineering: relics or resources?. *Australian Journal of Multi-Disciplinary Engineering* **2019** *15(1):100-11*

[14] Yang J, Xiang F, Li R, Zhang L, Yang X, Jiang S, Zhang H, Wang D, Liu X. Intelligent bridge management via big data knowledge engineering. *Automation in Construction* **2022** *135:104118*

[15] Nasr A, Kjellström E, Björnsson I, Honfi D, Ivanov OL, Johansson J. Bridges in a changing climate: A study of the potential impacts of climate change on bridges and their possible adaptations *Structure and Infrastructure Engineering* **2020** *16(4):738-49*

[16] Mendoza-Lugo MA, Nogal M, Morales-Nápoles O. Estimating bridge criticality due to extreme traffic loads in highway networks *Engineering Structures* **2024** *300:117172*

[17] Fussell J, Rundquist D, Harrington JA. On defining remote sensing. *Photogrammetric Engineering and Remote Sensing* **1986** *52(9):1507-11*

[18] Joseph G. Fundamentals of remote sensing. *Universities press* **2005**

[19] Andersen HE, Reutebuch SE, McGaughey RJ. Active remote sensing. InComputer Applications in Sustainable Forest Management: Including Perspectives on Collaboration and Integration **2006** *43-66 Dordrecht: Springer Netherlands*

[20] Chen SE, Liu W, Dai K, Bian H, Hauser E. Remote sensing for bridge monitoring. InCondition, Reliability, and Resilience Assessment of Tunnels and Bridges **2011** *118-125*

[21] Liu JG, Mason PJ. Image processing and GIS for remote sensing: techniques and applications *John Wiley and Sons* **2016**

[22] Abbasi T, Shams V, Azari B, Shamshirdar F, Baltes J, Sadeghnejad S. Inter-humanoid robot interaction with emphasis on detection: A comparison study–Addendum *The Knowledge Engineering Review* **2017** *32*

[23] Rosenqvist Å, Milne A, Lucas R, Imhoff M, Dobson C. A review of remote sensing technology in support of the Kyoto Protocol *Environmental Science and Policy* **2003** *6(5):441-55*

[24] Kaartinen E, Dunphy K, Sadhu A. LiDAR-based structural health monitoring: Applications in civil infrastructure systems. *Sensors* **2022** *22(12):4610*

[25] Jia J, Sun H, Jiang C, Karila K, Karjalainen M, Ahokas E, Khoramshahi E, Hu P, Chen C, Xue T, Wang T. Review on active and passive remote sensing techniques for road extraction. *Remote Sensing* **2021** *13(21):4235*

[26] Abdelmajeed AY, Juszczak R. Challenges and Limitations of Remote Sensing Applications in Northern Peatlands: Present and Future Prospects. *Remote Sensing* **2024** *16(3):591*

[27] Soergel, U.; Thiele, A.; Gross, H.; Thoennessen, U. Extraction of bridge features from high-resolution InSAR data and optical images. In Proceedings of the 2007 Urban Remote Sensing Joint Event, Paris, France, 11–13 April 2007; pp. 1–6.

[28] Abraham, L.; Sasikumar, M. Analysis of satellite images for the extraction of structural features. *IETE Tech. Rev.* **2014**, *31*, 118–127.

[29] Nettis, A.; Massimi, V.; Nutricato, R.; Nitti, D.O.; Samarelli, S.; Uva, G. Satellite-based interferometry for monitoring structural deformations of bridge portfolios. *Autom. Constr.* **2023**, *147*, 104707.

[30] Macchiarulo, V.; Milillo, P.; Blenkinsopp, C.; Giardina, G. Monitoring deformations of infrastructure networks: A fully automated GIS integration and analysis of InSAR time-series. *Struct. Health Monit.* **2022**, *21*, 1849–1878.

[31] Cusson, D.; Rossi, C.; Ozkan, I.F. Early warning system for the detection of unexpected bridge displacements from radar satellite data. *J. Civ. Struct. Health Monit.* **2021**, *11*, 189–204.

[32] Aswathi, J.; Binojkumar, R.B.; Oommen, T.; Bouali, E.H.; Sajinkumar, K.S. InSAR as a tool for monitoring hydropower projects: A review. *Energy Geosci.* **2022**, *3*, 160–171.

[33] Mcfeeters, S.K. The use of the Normalized Difference Water Index (NDWI) in the delineation of open water features. *Int. J. Remote Sens.* **1996**, *17*, 1425–1432.

[34] Sovisoth, E.; Kuntal, V.S.; Misra, P.; Takeuchi, W.; Nagai, K. Estimation of Year of Construction of Bridges in Cambodia by Analyzing the Landsat Normalized Difference Water Index. *Infrastructures* **2023**, *8*, 77.

[35] Srikanth I, Arockiasamy M. Deterioration models for prediction of remaining useful life of timber and concrete bridges: A review. *Journal of traffic and transportation engineering* **2020** *7(2):152-73*

[36] Kashiwa, T.; Nagai, K. Analysis of Bridge Inspection Data for the Strategic Infrastructure Management in Rural City in Japan, the 2nd ACF Symposium, 2017

[37] Mcfeeters, S.K. The use of the Normalized Difference Water Index (NDWI) in the delineation of open water features. *Int. J. Remote Sens.* **1996**, *17*, 1425–1432.

[38] Lefebvre, D.; Willm, C.; Redmond, M.; Guelmami, P. Introducing WIW for detecting the presence of water in wetlands with landsat and sentinel satellites. *Remote Sens.* **2019**, *11*, 257–266.

[39] Rodionov, S.N. A sequential method for detecting regime shifts in the mean and variance. In Large-Scale Disturbances (Regime Shifts) and Recovery in Aquatic Ecosystems: Challenges for Management toward Sustainability, $Publisher, UNESCO - ROSTE/BASWorkshoponRegimeShifts, 14 - 16June2005, Varna, Bulgaria$; 2005; pp. 68–72.

[40] Japan Meteorological Agency. Available online: `https://www.data.jma.go.jp/gmd/cpd/longfcst/en/tourist.html` (accessed on 25 January 2023).

[41] Nago City Population Statistics. Available online: `https://www.citypopulation.de` (accessed on 24 January 2023).

[42] National Road Facility Inspection Database for Japan. Available online: `https://road-structures-map.mlit.go.jp/FacilityList.aspx` (accessed on 21 December 2022).

[43] Landsat Science. Available online: `https://landsat.gsfc.nasa.gov/` (accessed on 21 December 2022).

[44] Laake, A. Electromagnetic spectral bands used for remote Sensing. *Remote. Sens. Hydrocarb. Explor,* $doi.org/10.1007/978 - 3 - 030 - 73319 - 3_2$ **2022**, 21–35.

[45] Prasad, A.D.; Ganasala, P.; Hernández-Guzmán, R.; Fathian, F. Remote sensing satellite data and spectral indices: An initial evaluation for the sustainable development of an urban area. *Sustain. Water Resour. Manag.* **2022**, *8*, 19.

[46] Rouse, J.W., Jr.; Haas, R.H.; Schell, J.A.; Deering, D.W. Monitoring vegetation systems in the Great Plains with ERTS. *NASA* **1974**, *1*, 9.

[47] Tucker, C.J.; Justice, C.O.; Prince, S.D. Monitoring the grasslands of the Sahel 1984–1985. *Int. J. Remote Sens.* **1986**, *7*, 1571–1581.

[48] Wang, F.; Huang, J.; Tang, Y.; Wang, X. New Vegetation Index and Its Application in Estimating Leaf Area Index of Rice. *Rice Sci.* **2007**, *14*, 195–203.

[49] Gao, B. NDWI—A Normalized Difference Water Index for remote sensing of vegetation liquid water from space. *Remote Sens. Environ.* **1996**, *58*, 257–266.

[50] Ozelkan, E. Water body detection analysis using NDWI indices derived from landsat-8 OLI. *Pol. J. Environ. Stud.* **2020**, *29*, 1759–1769.

[51] Xu, H. Modification of Normalized Difference Water Index (NDWI) to enhance open water features in remotely sensed imagery. *Int. J. Remote Sens.* **2006**, *27*, 3025–3033.

[52] Normalized Difference Snow Index. Available online: `https://www.usgs.gov/landsat-missions/normalized-difference-snow-index` (accessed on 22 January 2023).

[53] Normalized Difference Burn Ratio 2 Index. Available online: `https://www.usgs.gov/landsat-missions/landsat-normalized-burn-ratio-2` (accessed on 21 January 2023).

[54] Deng, Y.; Wu, C.; Li, M.; Chen, R. RNDSI: A ratio normalized difference soil index for remote sensing of urban/suburban environments. *Int. J. Appl. Earth Obs. Geoinf.* **2015**, *39*, 40–48.

[55] Rasul, A.; Balzter, H.; Ibrahim, G.; Hameed, H.; Wheeler, J.; Adamu, B.; Ibrahim, S.; Najmaddin, P. Applying built-up and bare-soil indices from Landsat 8 to cities in dry climates. *Land* **2018**, *7*, 81.

[56] Zha, Y.; Gao, J.; Ni, S. Use of normalized difference built-up index in automatically mapping urban areas from TM imagery. *Int. J. Remote Sens.* **2003**, *24*, 583–594.

[57] He, C.; Shi, P.; Xie, D.; Zhao, Y. Improving the normalized difference built-up index to map urban built-up areas using a semiautomatic segmentation approach. *Remote Sensing Letters* **2010**, *1(4)*, 213–221.

[58] Huang, C.; Thomas, N.; Goward, S.N.; Masek, J.G.; Zhu, Z.; Townshend, J.R.G.; Vogelmann, J.E. Automated masking of cloud and cloud shadow for forest change analysis using Landsat images. *Int. J. Remote Sens.* **2010**, *31*, 5449–5464.

[59] Candra, D.S.; Phinn, S.; Scarth, P. Cloud and cloud shadow masking using multitemporal cloud masking algorithm in tropical environment. *Int. Arch. Photogramm. Remote Sens. Spat. Inf. Sci.* **2016**, *XLI-B2*, 95–100.

[60] Rodionov, S.N. A sequential algorithm for testing climate regime shifts. *Geophysical Research Letters, Wiley Online Library* **2004**, *31(9)*.

[61] Rodionov, S.N. A brief overview of the regime shift detection methods. In *Large-Scale Disturbances (Regime Shifts) and Recovery in Aquatic Ecosystems: Challenges for Management toward Sustainability*; 2005; pp. 17–24.

[62] Rodionov, S.N.; Overland, J.E. Application of a sequential regime shift detection method to the Bering Sea ecosystem. *ICES J. Mar. Sci.* **2005**, *62*, 328–332.

[63] Van den Burg, G.J.J.; Williams, C.K.I. An evaluation of change point detection algorithms. *arXiv* **2020**, arXiv:2003.06222.

[64] Landsat Collection 1 vs. Collection 2 Summary U.S. Geological Survey. Available online: https://www.usgs.gov/landsat-missions/news/landsat-7-nominal-science-mission-ending (accessed on 22 December 2022).

[65] Landsat Full Resolution Browse Images U.S. Geological Survey. Available online: https://www.usgs.gov/landsat-missions/landsat-full-resolution-browse-images (accessed on 22 December 2022).

[66] The 2021 Annual Report. Road Development Agency. Available online: https://www.rda.org.zm/wp-content/uploads/2023/09/RDA-Annual-Report-2021.pdf (accessed on 01 December 2023).

[67] Bridge Maintenance Capacity Building Project Report. JICA. Available online: https://openjicareport.jica.go.jp/pdf/12291886_01.pdf (accessed on 09 November 2023).

[68] The 2016 Annual Report. National Roads Funds Agency. Available online: https://nrfa.org.zm/wp-content/uploads/2019/01/annual-report-2016.pdf (accessed on 13 November 2023).

[69] Goma J.M. The Challenges of Road Construction in Zambia's Western Province: A Case Study of the Mongu–Kalabo Road Project. *Journal of Civil Engineering and Architecture* **2022** *16*, 619-25.

[70] Zeller W. Danger and Opportunity in Katima Mulilo: A Namibian Border Boomtown at Transnational Crossroads. *Journal of Southern African Studies* **2009**, *35(1)*, 133-54.

[71] The 2009 Chirundu Border Post Report [Internet]. Sub-Saharan Africa Transport Policy Program. Available online: https://www.ssatp.org/sites/ssatp/files/publications/SSATP-DiscussionPapers/DP10-Chirundu.pdf (accessed on 01 December 2023).

[72] Reinholdt P., Veje E., Kalvslund J. Rehabilitation of the Luangwa Bridge. *In Proceedings of the IABSE Conference, Cable-Stayed Bridges, Past, Present, and Future, Malmo, Sweden* **1999**

[73] Billington D.P., Nazmy A. History and Aesthetics of Cable-Stayed Bridges. *Journal of Structural Engineering* **1991** *117(10)*, 3103-34.

[74] The 2016 Annual Report [Internet]. National Roads Funds Agency. Available online: https://nrfa.org.zm/wp-content/uploads/2019/01/Annual-Report-2014.pdf (accessed on 01 December 2023).

[75] Victoria Falls Bridge. American Society of Civil Engineers. Available online: https://www.asce.org/about-civil-engineering/history-and-heritage/historic-landmarks/victoria-falls-bridge (accessed on 01 December 2023).

[76] The Feasibility Study on the Kafue road bridge Reconstruction Project in the Republic of Zambia, JICA. Available online: https://openjicareport.jica.go.jp/615/615/615_533_10897866.html (accessed on 01 December 2023).